Lasers:
Statistical mechanics in nonlinear optics and photonics

Claudio Conti
Institute for Complex Systems
National Research Council
www.complexlight.org

Cortona, Netadis meeting, 10-11 Luglio 2014

Nonlinear optics and photonics

- Nonlinear Optics
  - Progagation of light beams and light pulses
- Photonics
  - Light-matter interaction
  - Lasers

Outline

- Today
  - Nonlinear optics
- Tomorrow
  - Photonics (lasers)

In other words

- Nonlinear optics
  - Hamiltonian systems
- Photonics
  - Dissipative systems (gain and loss)

(“Extreme”) Nonlinear optics

Some modern topics

Propagation of light in the atmosphere

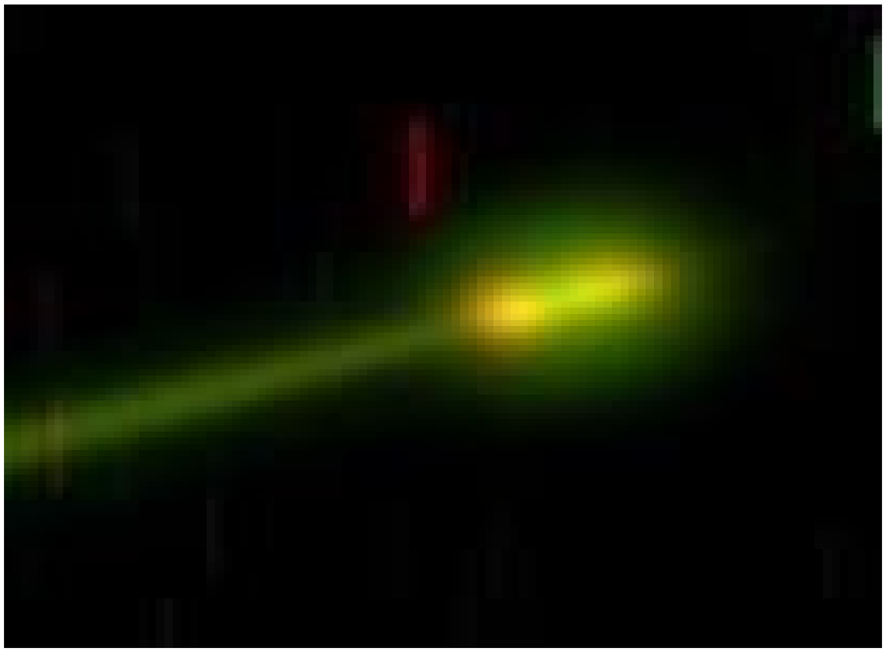

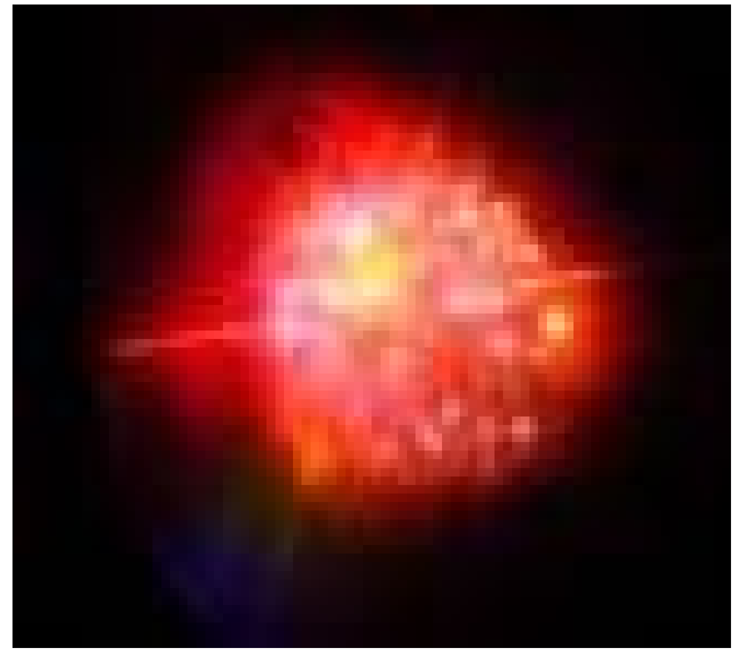

A femtosecond laser pulse with TW of peak power propagates for kilometers

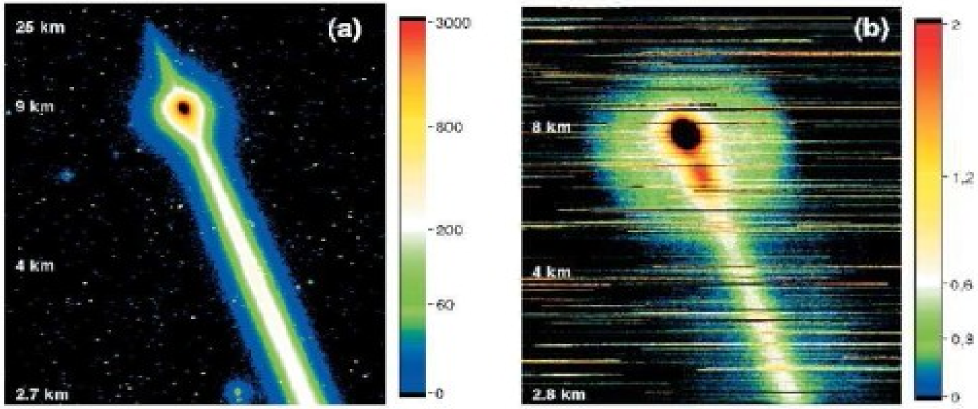

FIG. 25 Typical fs beam image of the Teramobile laser beam from Tautenburg observatory. (a) Fundamental wavelength; (b) Blue-green band of the continuum. The horizontal stripes across the pictures come from stars passing through the telescope field of view. Note the strongly nonlinear altitude scale due to triangulation.

Above a critical power filaments can propagate for kilometers

Berge' et al, physics/0612063

The teramobile project

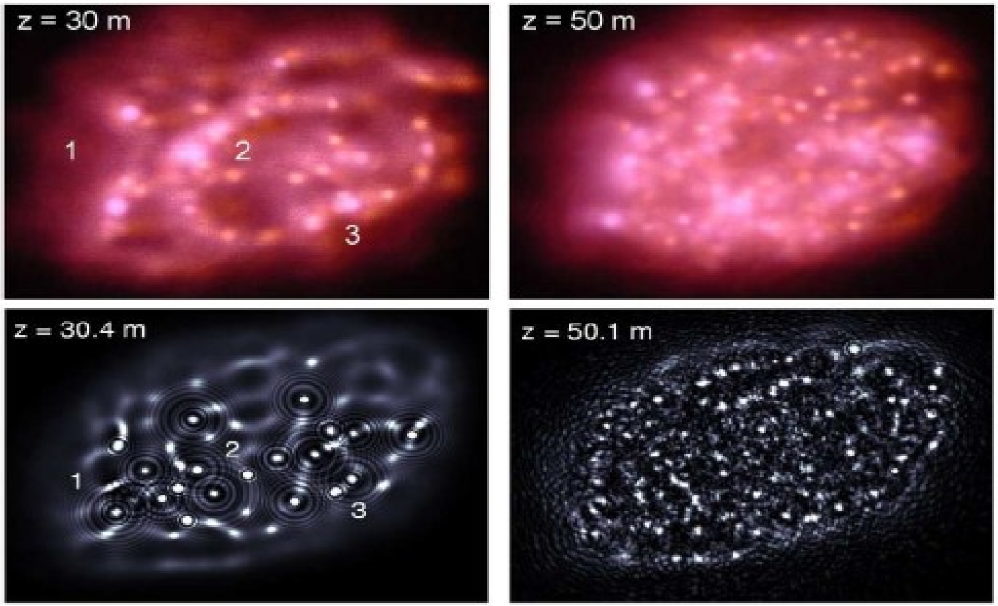

FIG. 28 Filamentation patterns from the Teramobile beam with $w_0 = 2.5$ cm, FWHM duration of 100 fs and input power equal to 700 $P_{\rm cr}$ at different distances z. (top) Experiments; (bottom) Numerical computations.

FIG. 30 Open cloud chamber. The cloud spans over 10 m.

Filaments through fog !

Berge' et al, physics/0612063

Filaments distribution depends on pressure and other parameters

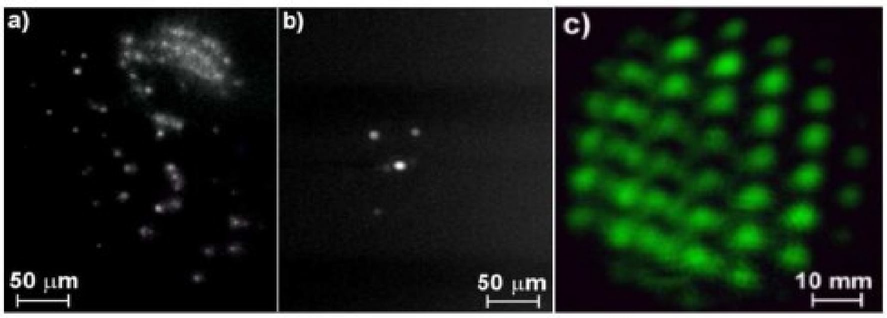

FIG. 24 Filamentation pattern obtained from a 1-cm long cell of (a) pure ethanol, (b) dilute solution of ethanol/Coumarin 153 at 4 g/l, (c) far-field fluence distribution of excited states of Coumarin emitting simultaneously in phase.

Berge' et al, physics/0612063

Filaments can go trhough obstacles

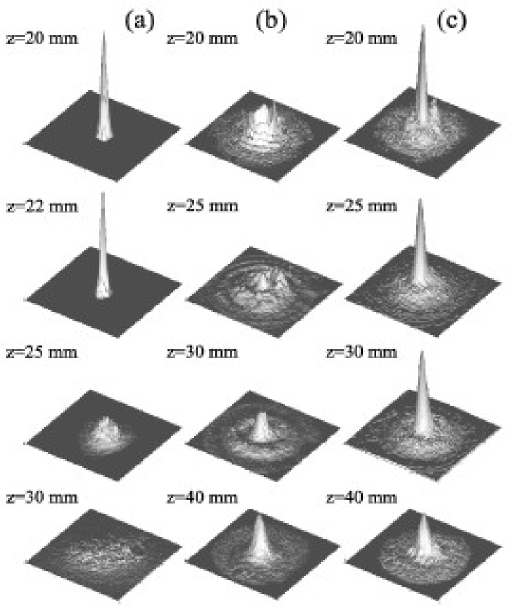

Dubietis et al PRL 2004 (water)

Phys. Rev. Focus, 4 September 2003

Laser induced lightings

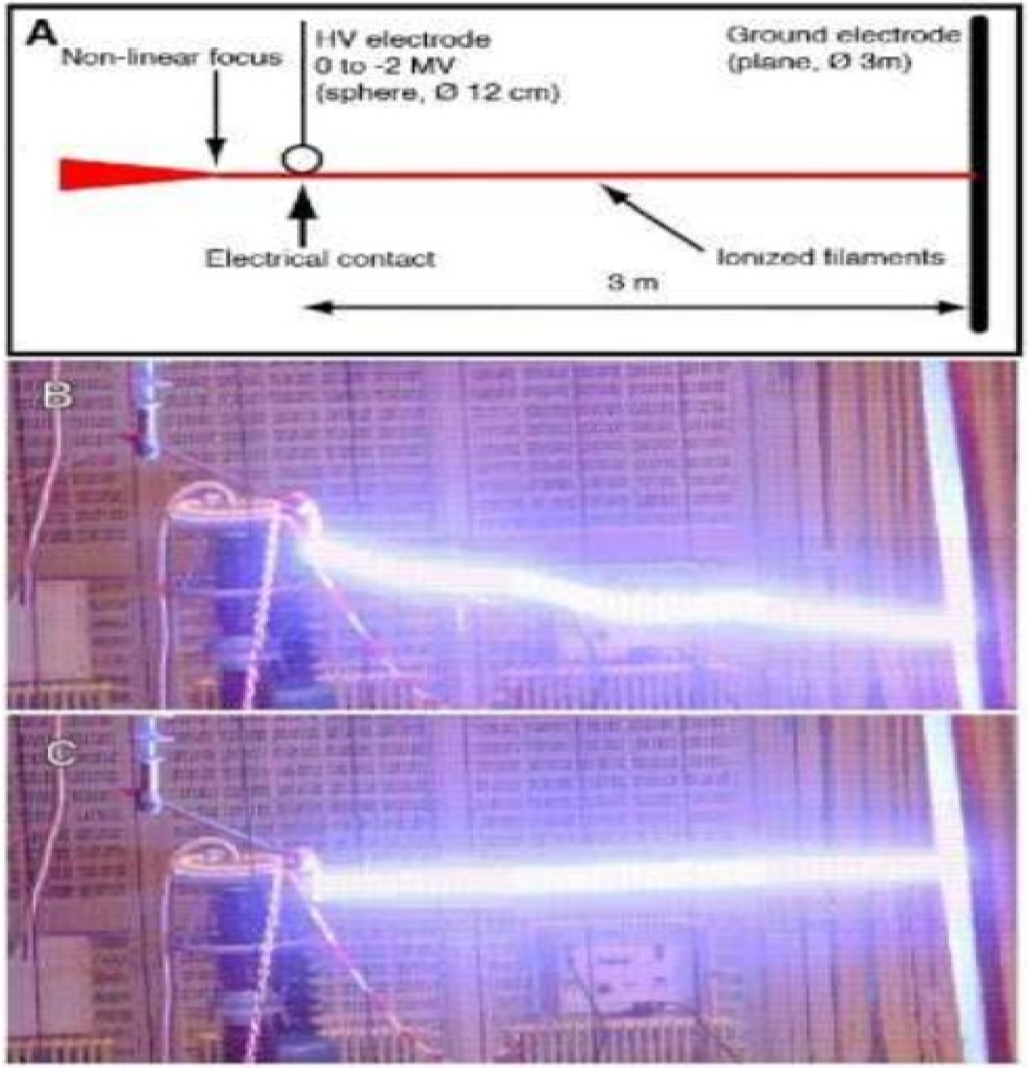

FIG. 37 Laser control of high-voltage discharges. (A) Experimental setup. (B) Free discharge over 3 m, without laser filaments. Note the erratic path. (C) Straight discharge guided along laser filaments (Kasparian et al., 2003).

Structures of the beam

- The filaments (3D+1 structures)

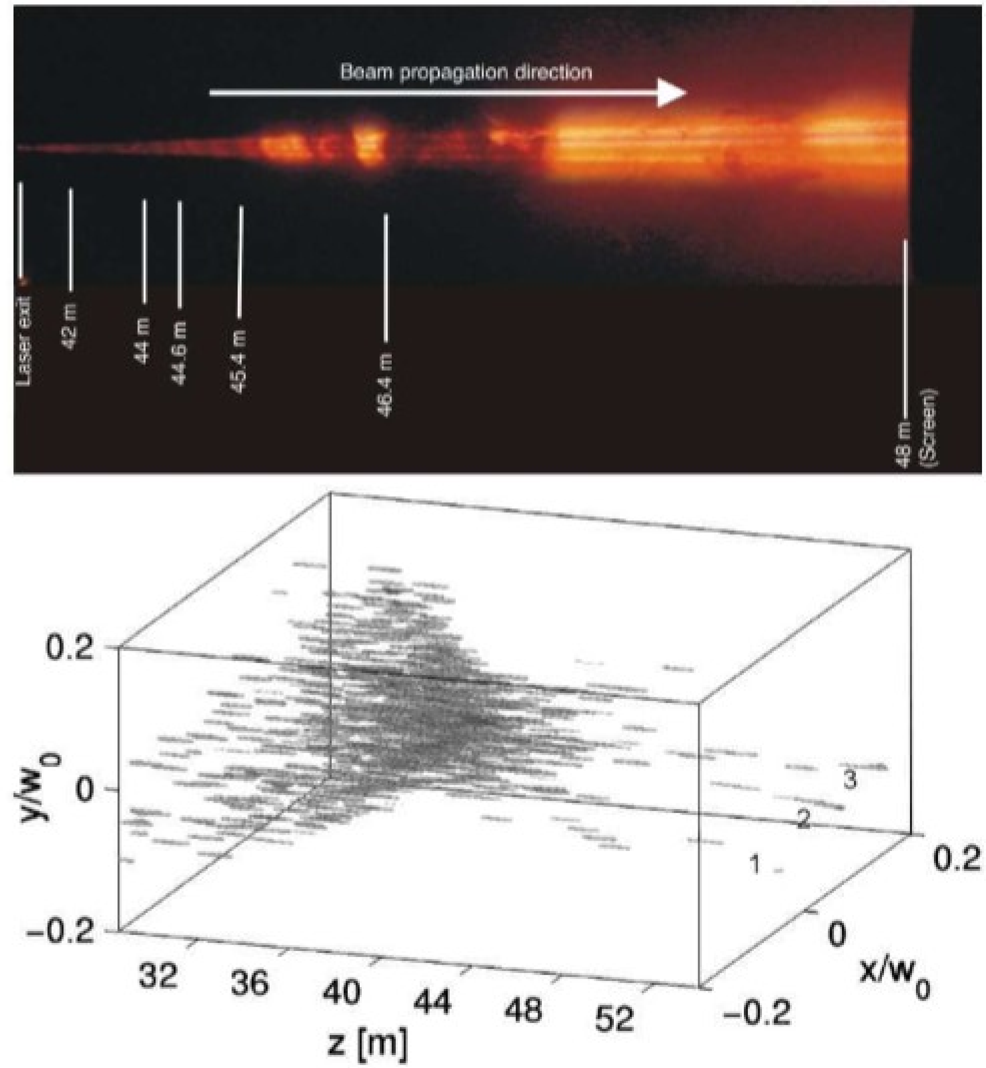

FIG. 29 Teramobile fluence of a focused beam (f = 40 m) with 760 critical powers, yielding three filamentary strings beyond the linear focal point: (top) Experiment, (bottom) numerical computation from the 2D model (71).

- “Swarming of filaments”
- Remark: in the process of filamentation there is time and space
- In fibers we have just time dynamics

Supercontinuum generation

Starting from a beam with narrow band, one generates white light

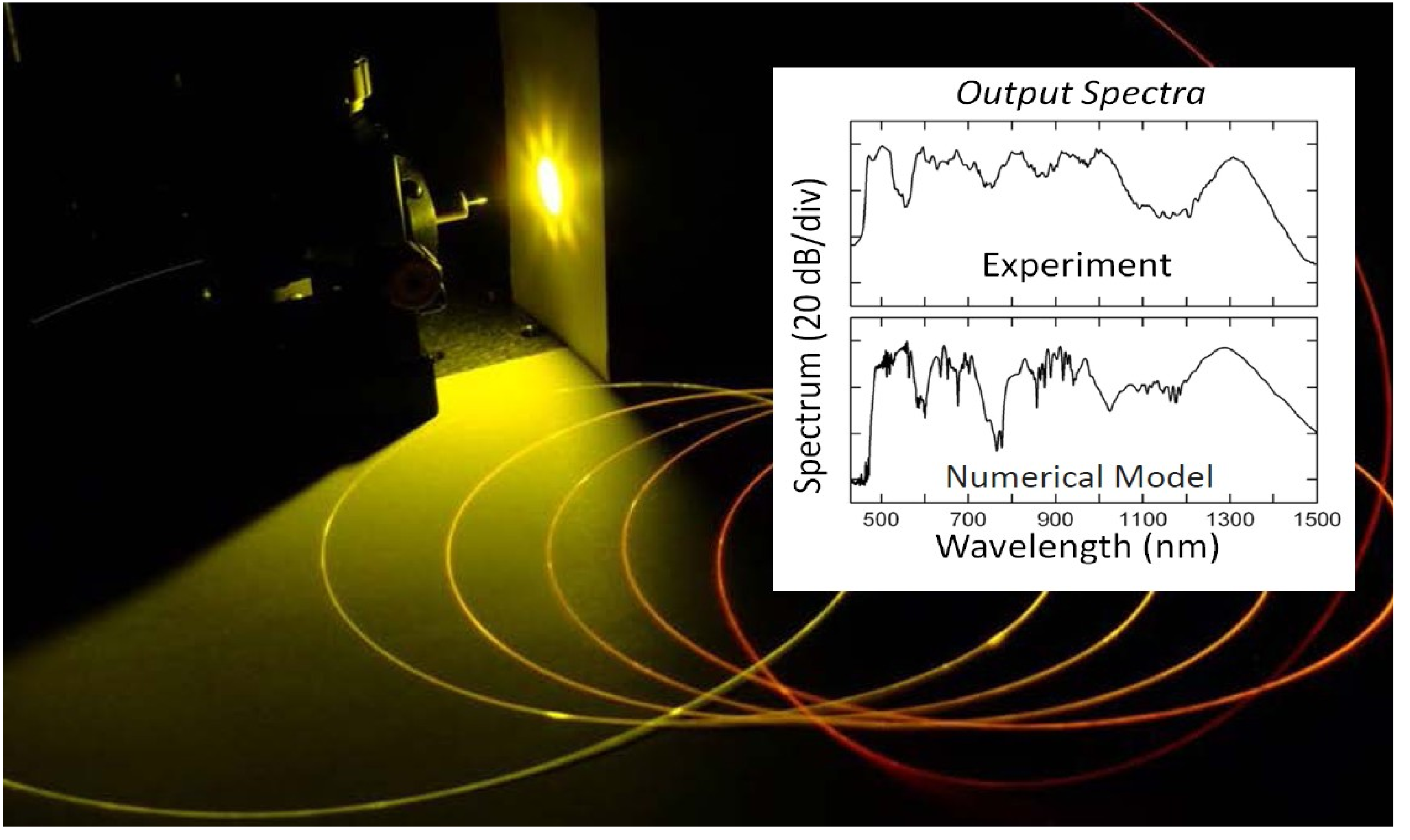

What happens in the time domain?

The temporal profile looks to be organized in specific particle-like wavepacket

These are the solitons

There are regime with hundreds of solitons

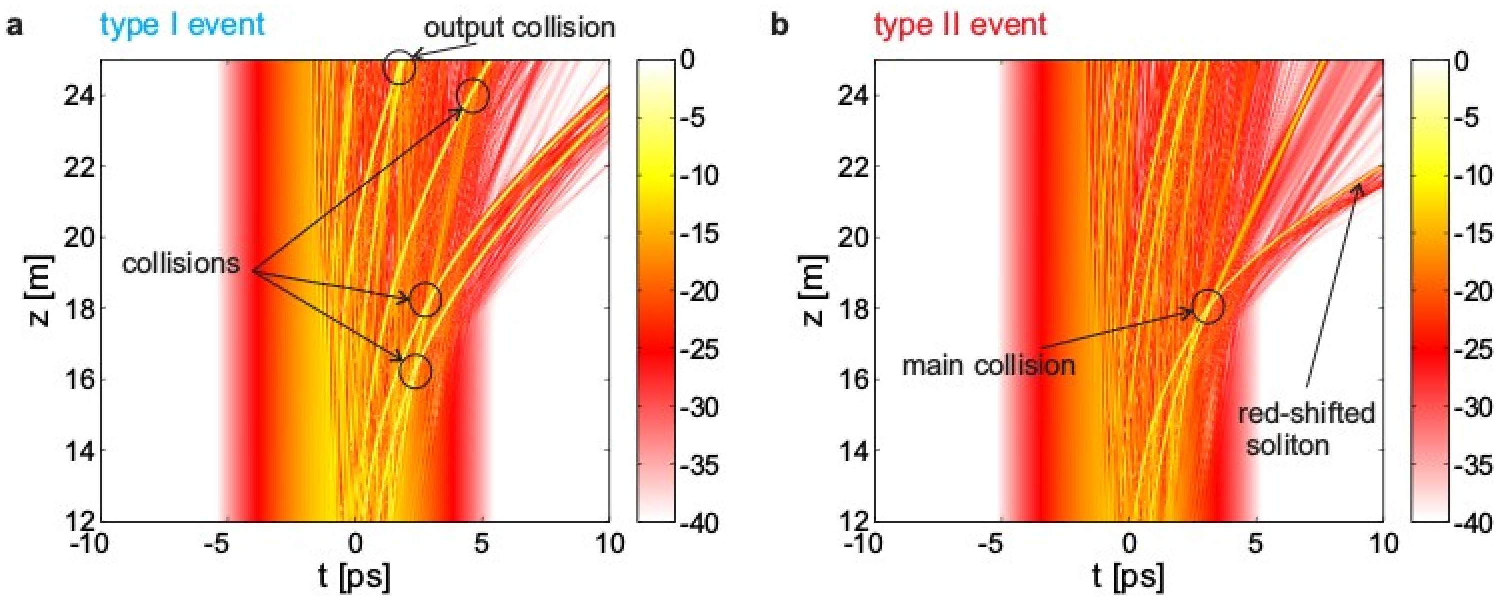

The interaction of solitons generated very particular events: rogue waves

Rogue waves (Oceanic)

Large ocean waves that appear in an otherwise calm sea

Large (~ 30 m) surface waves
that represent statistical outliers

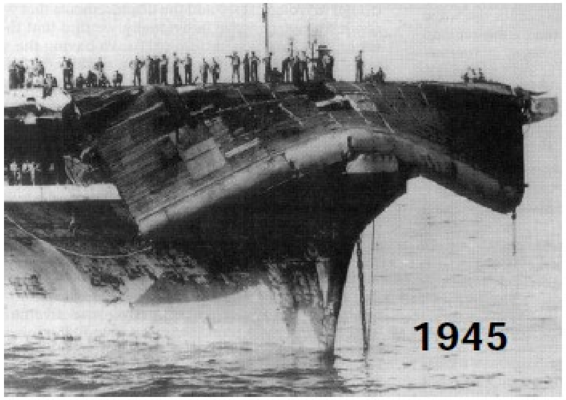

Measurements in 1990's have
established long-tailed statistics

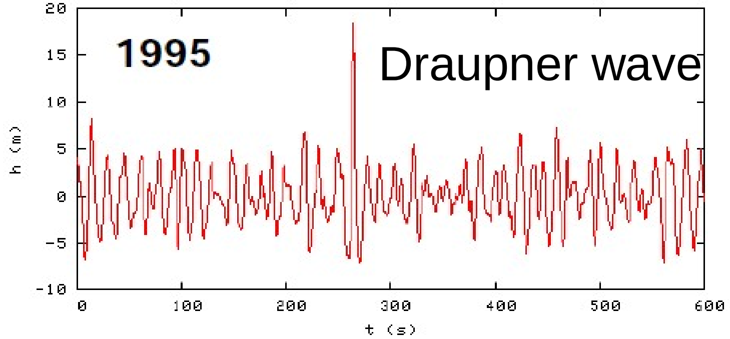

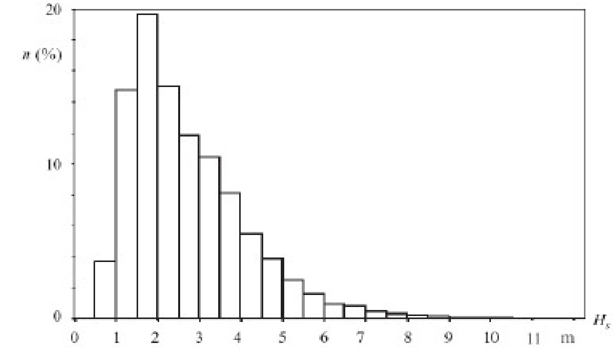

Figure 4.19 The histogram of the significant wave height for the years 1980–2003 for NODC buoy 46005 of Fig. 4.17 (n is the percentage of the total number of occurrences in the interval $\Delta H_s = 0.5$ m).

C. Kharif *et al. Rogue Waves in the Ocean*, Springer (2009)

Draupner platform Noth Sea
1 January 1995 (Wikipedia)

Rogue waves in optics

Modelling reveals that the supercontinuum can be highly unstable

$$\frac{\partial A}{\partial z} + \frac{\alpha}{2}A - \sum_{k\geq 2} \frac{\mathrm{i}^{k+1}}{k!}\beta_k \frac{\partial^k A}{\partial T^k} = i\gamma \left(1 + \mathrm{i}\tau_{\mathrm{shock}}\frac{\partial}{\partial T}\right)\left(A(z,t)\int_{-\infty}^{+\infty} R(T')|A(z,T-T')|^2 dT'\right)$$

Stochastic simulations

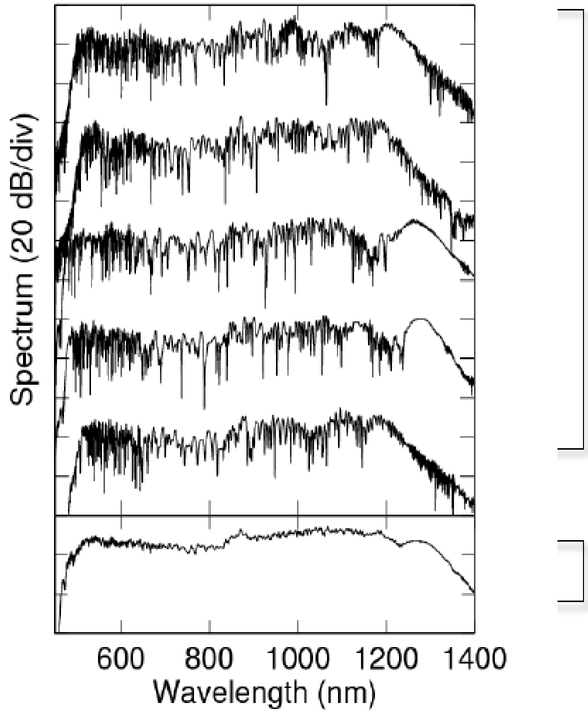

5 individual realisations, identical apart from quantum noise

Successive pulses from a laser pulse train generate significantly different spectra

We measure an artificially smooth spectrum, but the noise is still present

J. M. Dudley, G. Genty, S. Coen, Rev. Mod. Phys. 78 1135 (2006)

Experiments

Experiments reveal that these instabilities yield long-tailed statistics

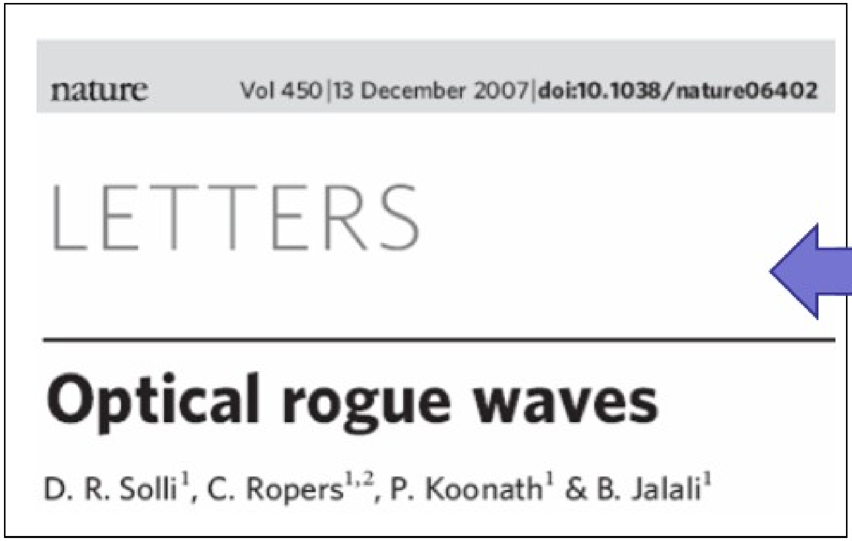
nature Vol 450 | 13 December 2007 | doi:10.1038/nature06402

LETTERS

Optical rogue waves

D. R. Solli[1], C. Ropers[1,2], P. Koonath[1] & B. Jalali[1]

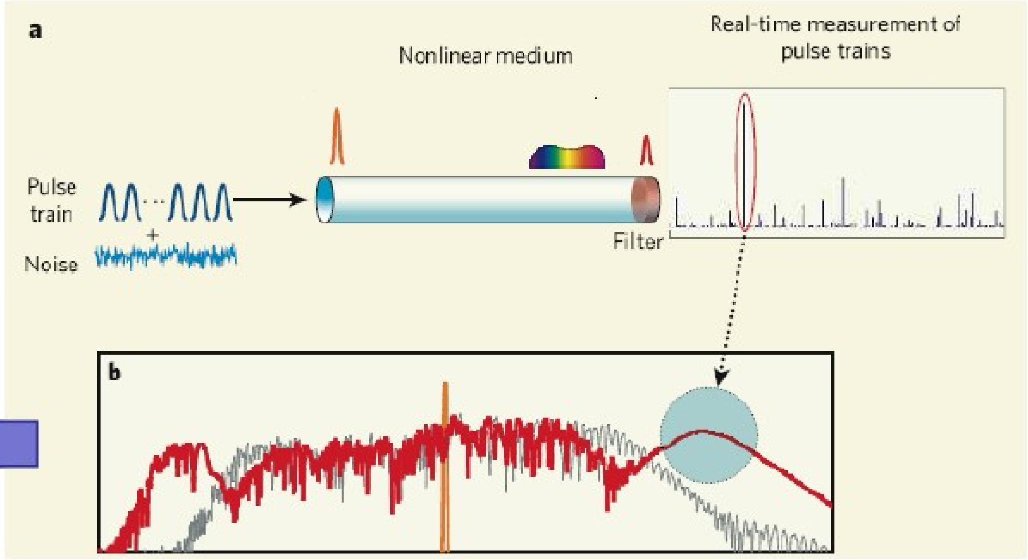

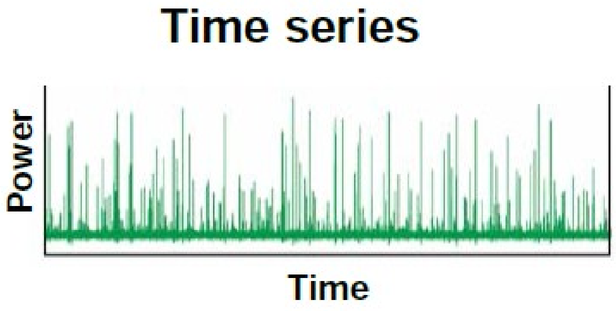

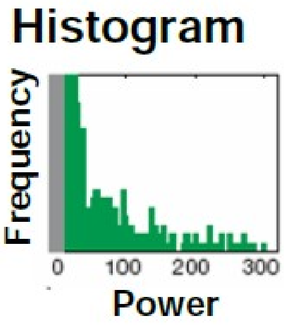

The program

- There is a series of highly nonlinear regimes
  - Filamentation
  - Supercontinuum generation
  - Rogue wave generation
  - Shock waves
  - Others...
- We want to describe these processes by using ideas from statistical mechanics

Let's start from scratch ...

$$\nabla^2 \mathcal{E} - \frac{n^2}{c^2}\frac{\partial^2 \mathcal{E}}{\partial t^2} = 0$$

The wave equation

The simplest solution: plane wave

$$\mathcal{E} = E\cos(\omega t - kz) = \Re[Ee^{-i\omega t + ikz}]$$

$$k = \frac{\omega n}{c} = \frac{2\pi n}{\lambda}$$

Harmonic fields

$$\mathcal{E} = \Re[E(x,y,z)e^{-i\omega t + ikz}]$$

$$\nabla^2 E + \omega^2 \frac{n^2}{c^2} E = 0$$

The Helmholtz equation

$$I = \frac{c\epsilon_0}{2}|E|^2 = |A|^2$$

Complex amplitude

The nonlinear refractive index

$$n = n_0 + \Delta n[|A|^2] = n_0 + \Delta n[I]$$

$$\Delta n = n_2 I$$

The paraxial approximation

$$2\imath k \frac{\partial A}{\partial z} + \nabla^2_{xy} A + 2k^2 \frac{\Delta n}{n_0} A = 0$$

$$\partial_y A = 0$$

$$2\imath k \frac{\partial A}{\partial z} + \frac{\partial^2 A}{\partial x^2} + 2k^2 \frac{n_2 |A|^2}{n_0} A = 0$$

The nonlinear Schroedinger equation

$$\imath \frac{\partial \psi}{\partial z} + \frac{\partial^2 \psi}{\partial x^2} + |\psi|^2 \psi = 0$$

$$\psi = 2\nu \,\mathrm{sech}[2\nu(x-\xi)] e^{2\imath\mu(x-\xi)+\imath\delta}$$

$$I(x) = 4\nu^2 \,\mathrm{sech}[2\nu(x-\xi)]^2$$

Diffraction and self-trapping

Beams tend to delocalize (spread) in space

Nonlinear effects trigger self-trapping

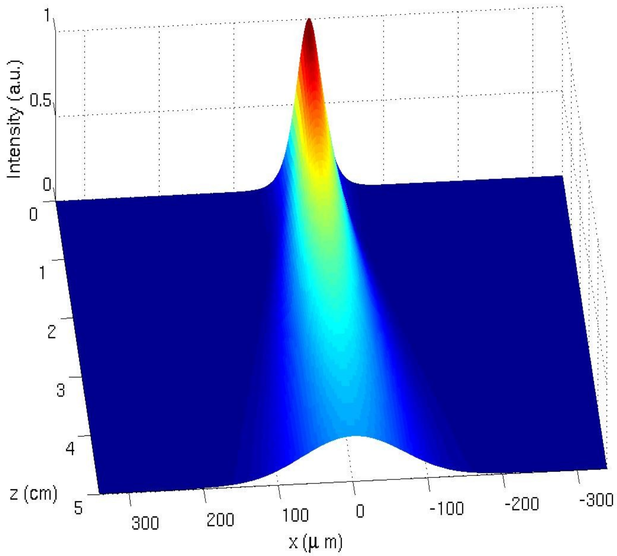

Low intesity = diffraction

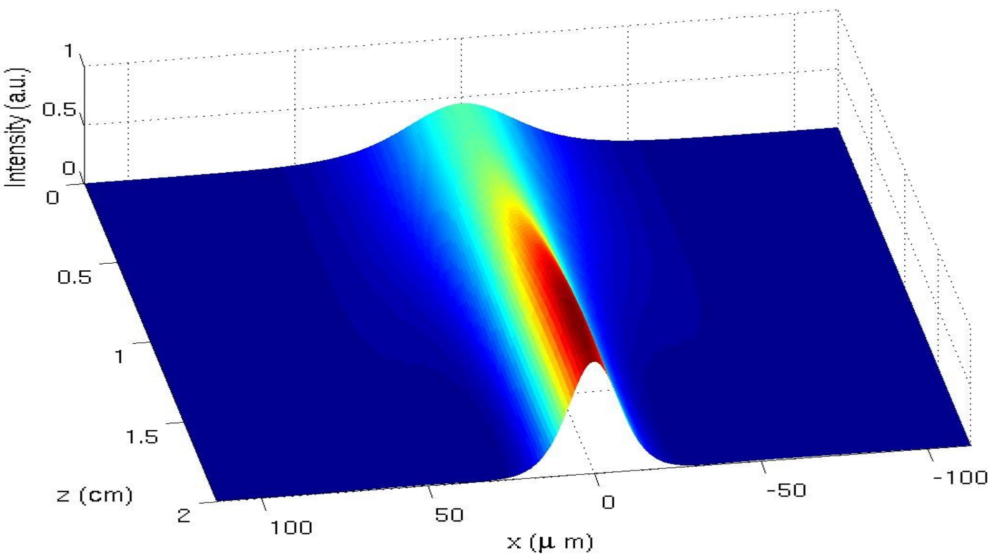

High intensity = self-trapping

The origin of self-trapping

Refractive index $n = n_0 + n_2 I$

$n_2 > 0$: focusing
$n_2 < 0$: defocusing

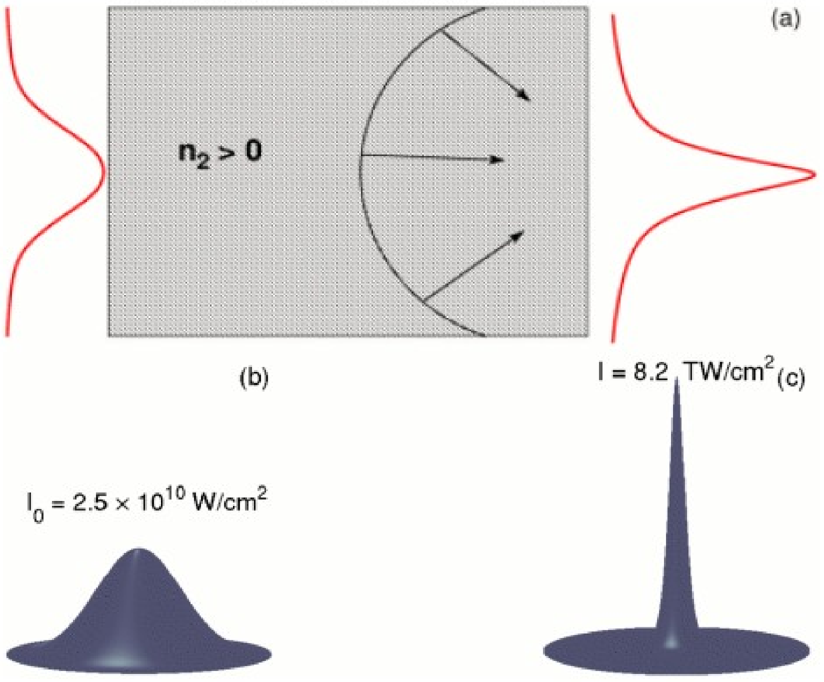

Berge' et al, physics/0612063

The nonlocal nonlinear refractive index

$$n(x) = n_0 + n_2 I(x)$$

$$n(x) = n_0 + \int_{-\infty}^{\infty} K(x - x')I(x')dx'$$

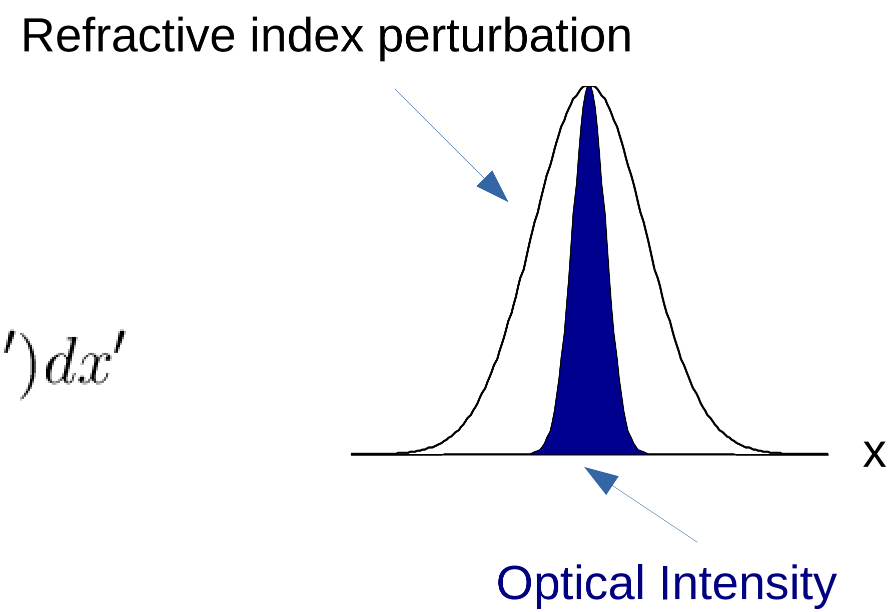

Introduction to nonlocal nonlinear optics

Well known ...

Nonlocal effects are known since the beginning of nonlinear optics (as the thermal effect, Shen Book)

“Nonlocal” temporal effects (Raman) in fibers were considered since 1967

The prediction of the collapse removal due to nonlocality is dated several decades ago (Turytsin 1985)

Optical spatial solitons

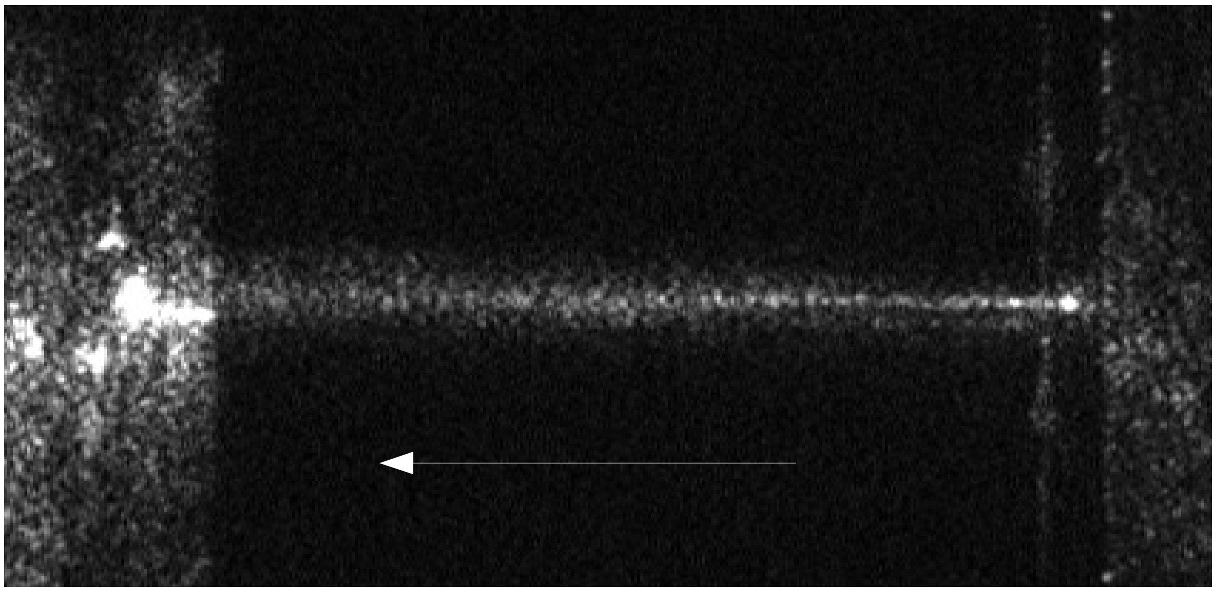

Diffracting beam

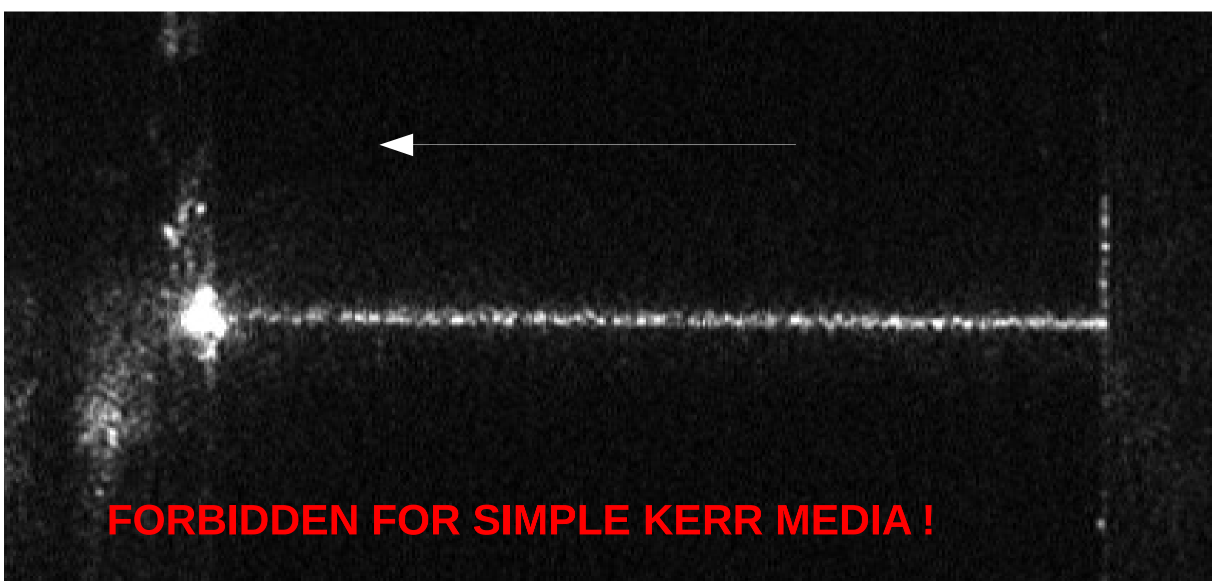

Optical spatial soliton

Catastrophic Self-focusing

Historically, the first reason for nonlocality

$$n(x) = n_0 + n_2 I(x)$$

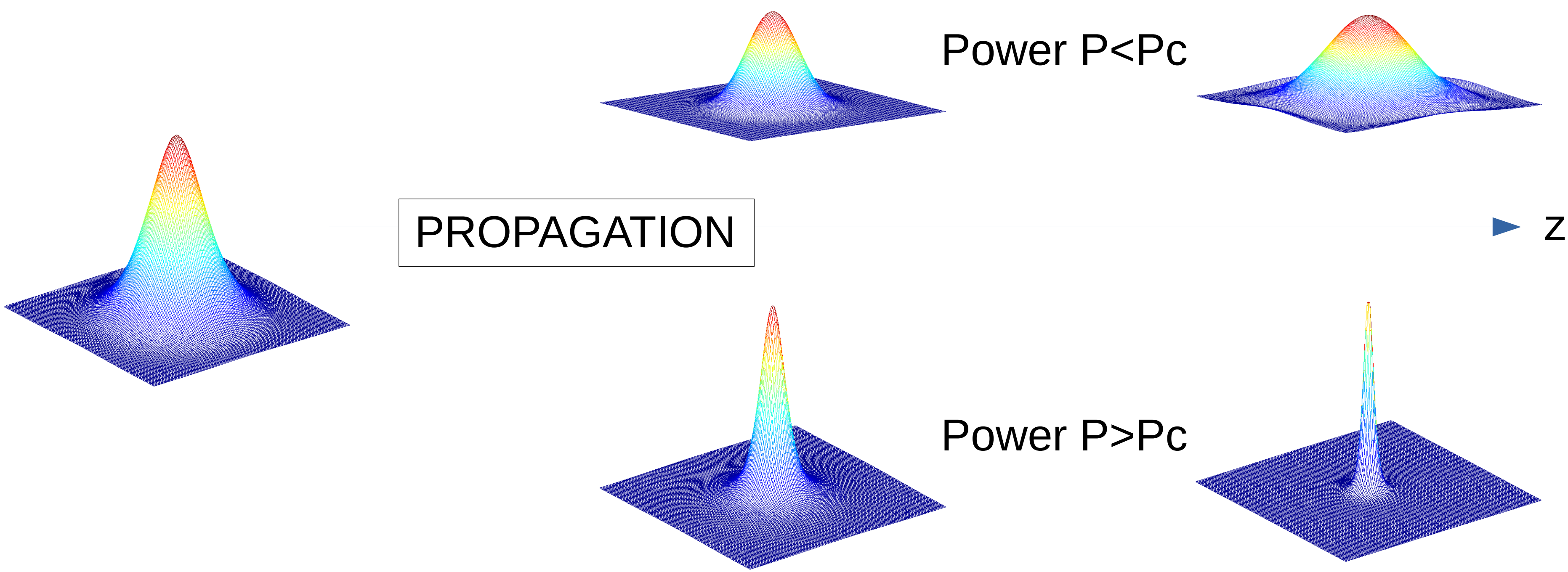

$$P_c = (0.61\lambda)^2 \pi/(8 n_0 n_2) \cong 2.6 \text{ MW}$$ for fused silica

Waist and Intensity Vs propagation

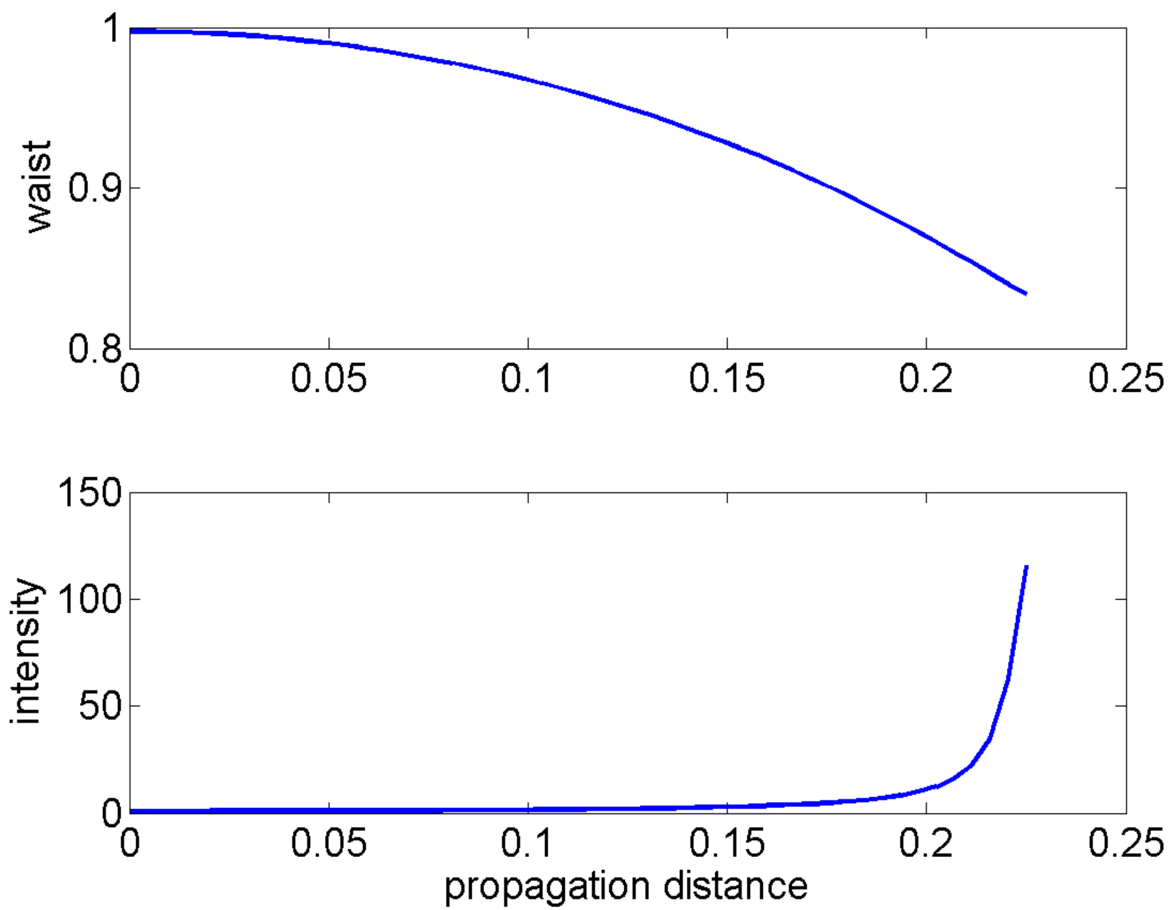

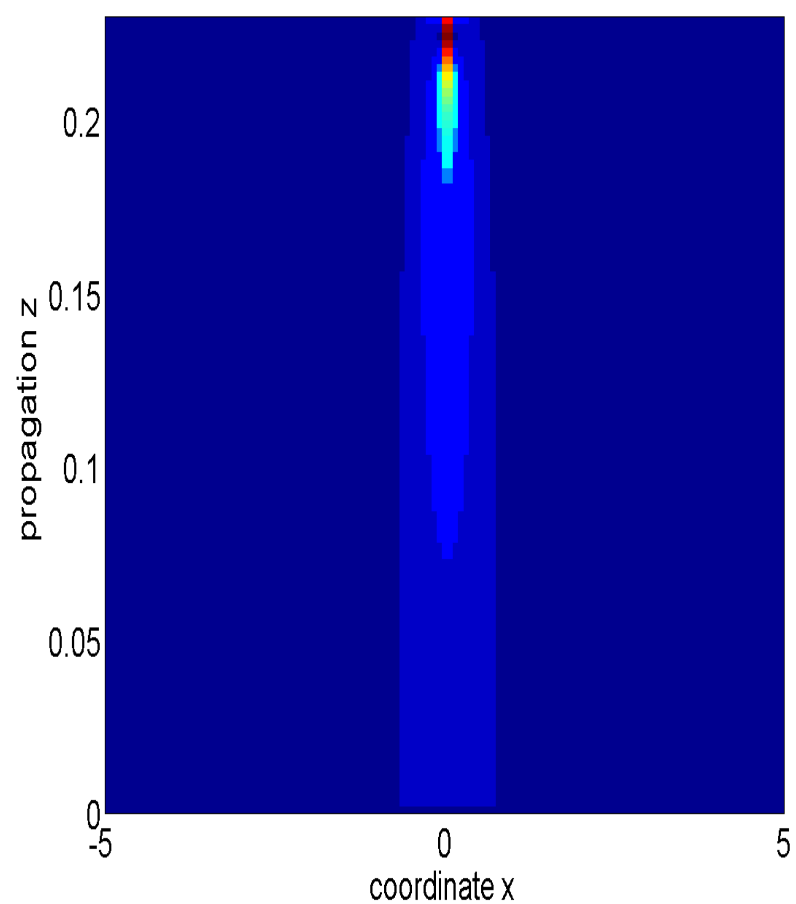

For a simple Kerr medium the beam evolves towards a singular solution

A strategy:
limit the waist

How to introduce a mechanism that intervenes only when the waist is small ?

By nonlocality !

Simple: spatial filtering

$$\Delta n(x,y) = \int_{-\infty}^{\infty} K(x-x', y-y')\, I(x',y')\, dx'\, dy'$$

Spatial domain

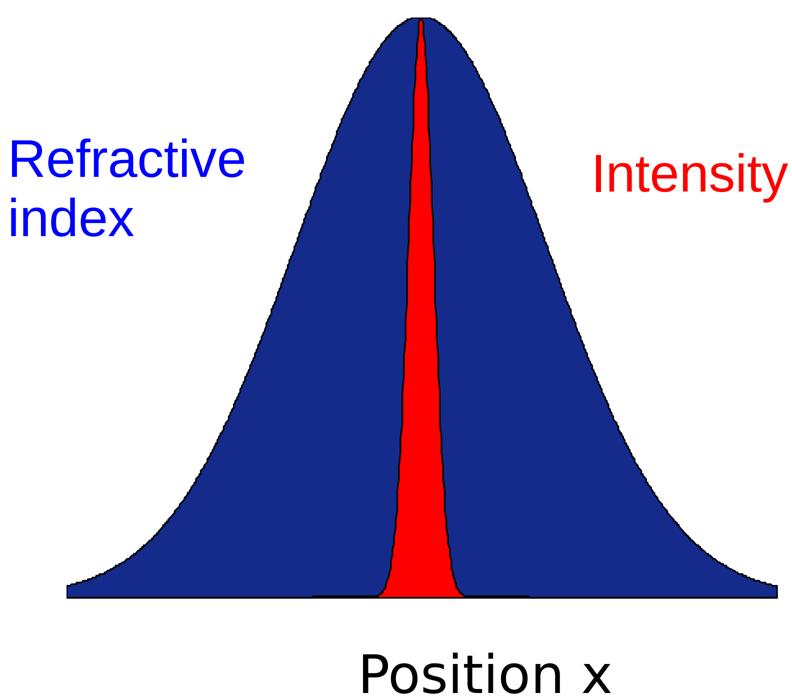

$$S(k_x,k_y) = \tilde{K}(k_x,k_y)$$

Wavenumber domain

$$\tilde{\Delta n}(k_x,k_y) = S(k_x,k_y)\, I(k_x,k_y)$$

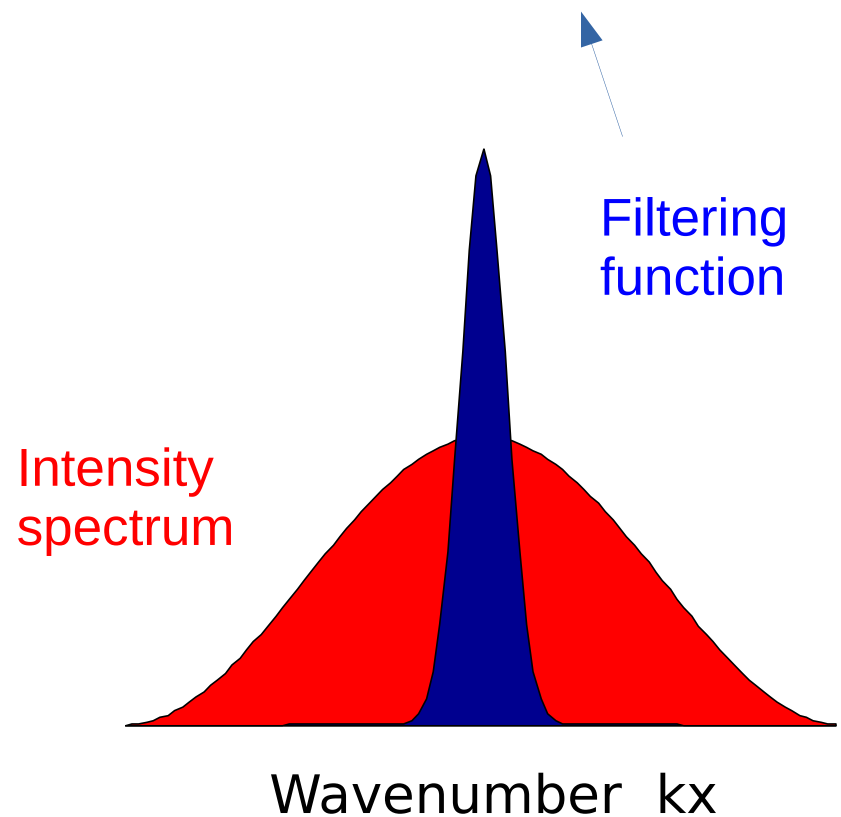

Collapse-free Nonlocal propagation

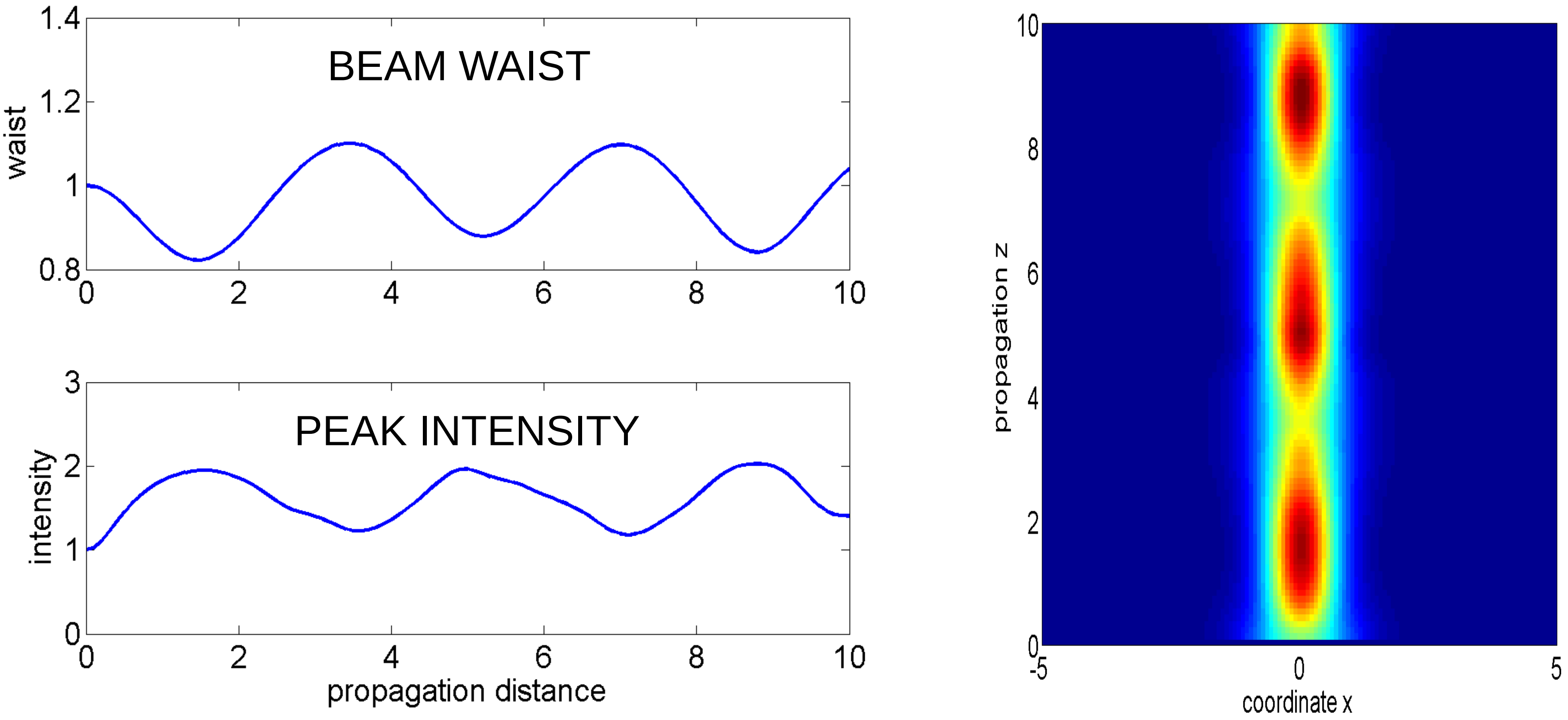

Recent paper by Maucher, Krolikowski and Skupin, arXiv:1008.1891

This filter action is more effective when the

“Degree of Nonlocality”

is higher

Degree of nonlocality

=

index waist/intensity waist

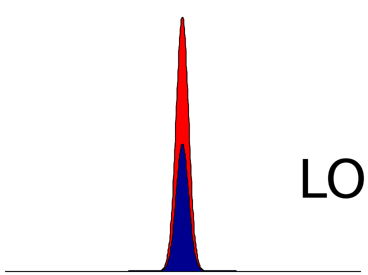

LOCAL

NON LOCAL

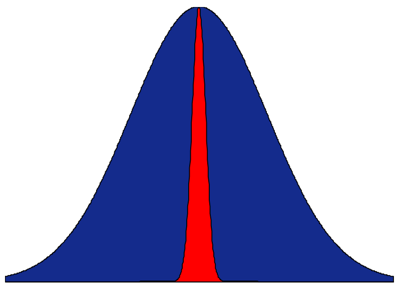

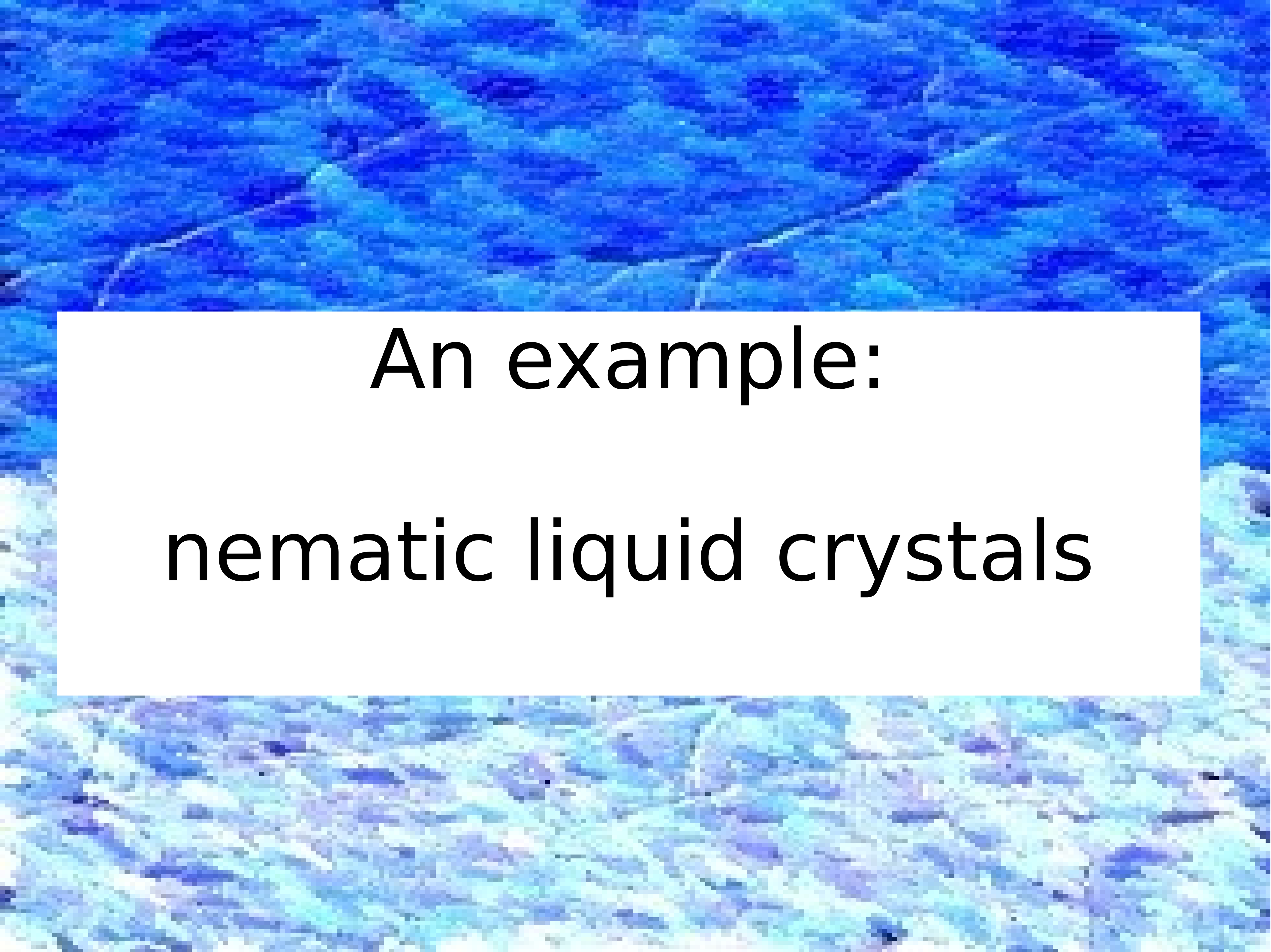

An example:

nematic liquid crystals

Re-orientational nonlinearity

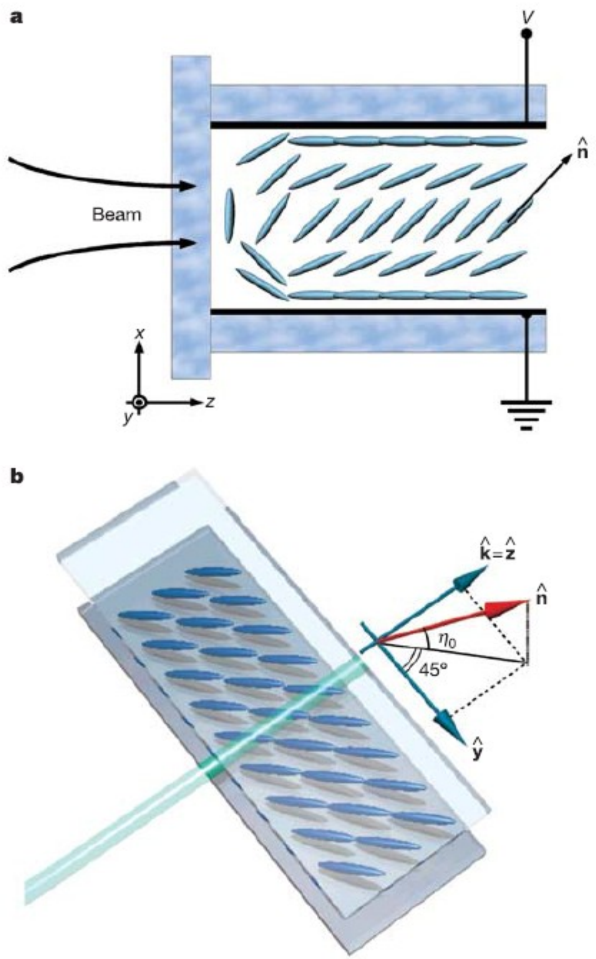

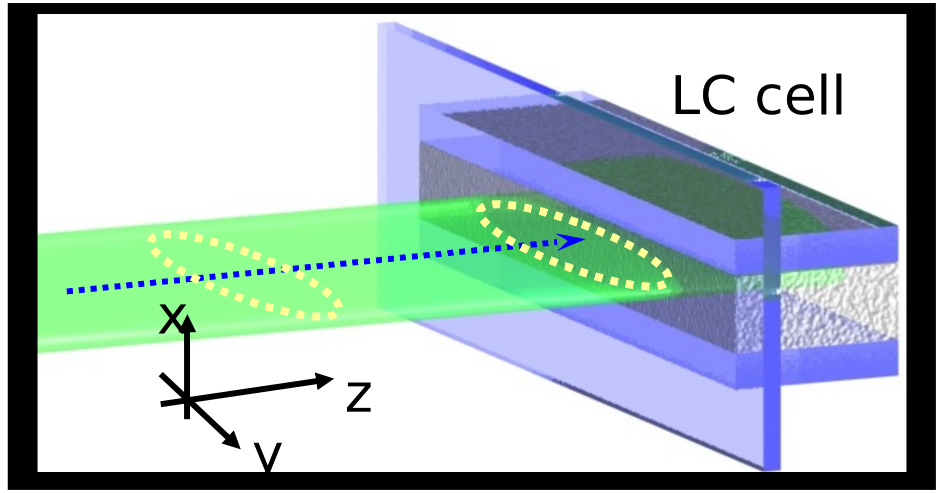

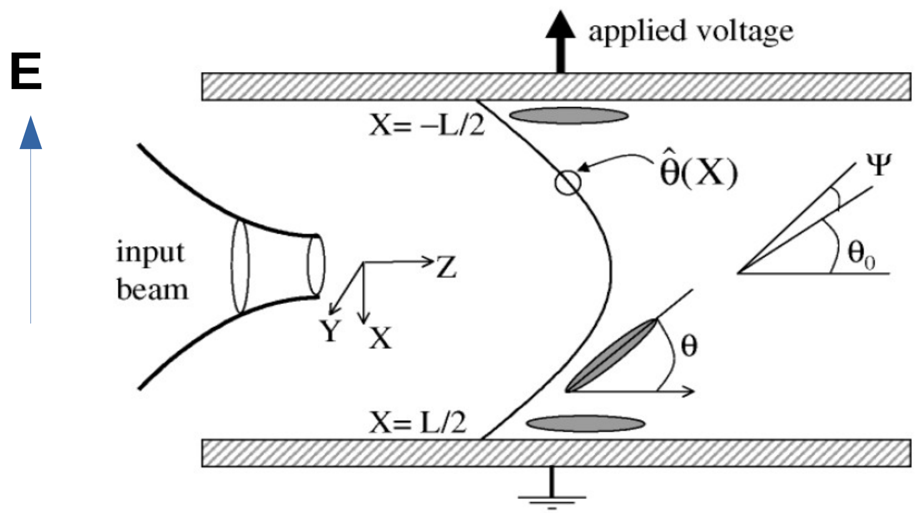

Peccianti, Conti, Assanto, et al Nature 432,733 2004

The model

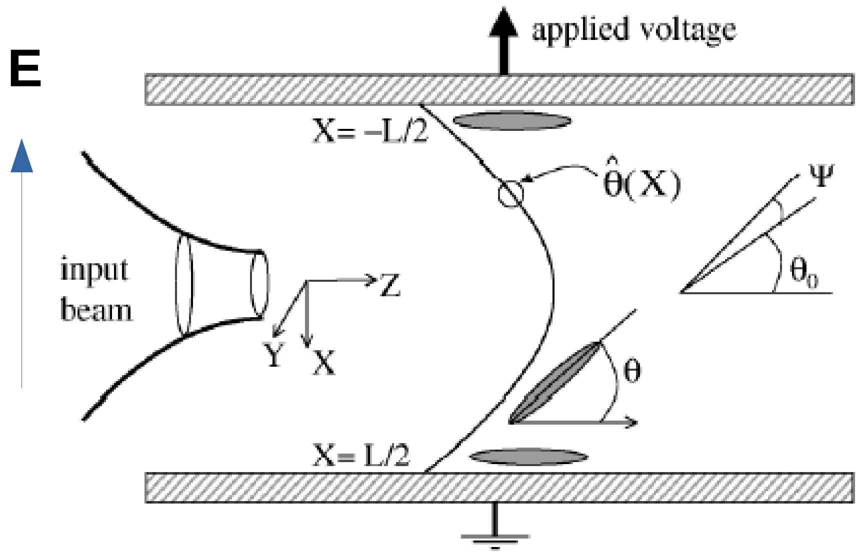

$$\Delta n = \frac{n_a^2}{2n_0}\Psi$$

$$K\nabla^2_{XYZ}\Psi - \frac{2\Delta\epsilon_{\mathrm{RF}}E^2}{\pi}\Psi + \frac{\epsilon_0 n_a^2}{4}|A|^2 = 0,$$

$$\tilde{\Psi} = \frac{1}{1+\sigma^2(k_x^2+k_y^2)}\tilde{I}$$

$$\sigma = \sqrt{\frac{\pi K d^2}{2\Delta\epsilon_{RF}V^2}}$$

Conti et al. PRL 91, 073901 (2003)

The degree of nonlocality

$$\tilde{\Delta} n(k_x, k_y) = \frac{n_2}{1 + \sigma^2 (k_x^2 + k_y^2)} \tilde{I}(k_x, k_y)$$

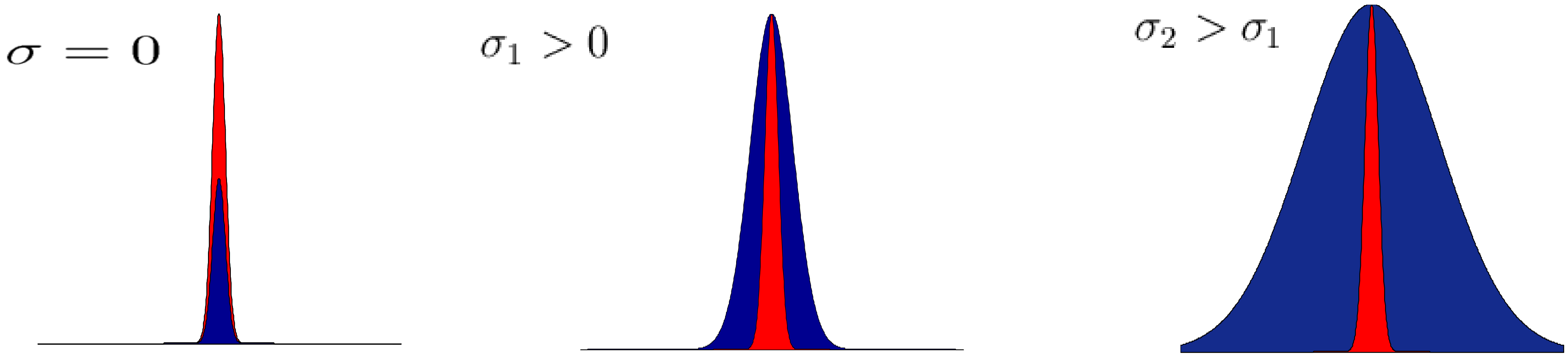

In liquid crystals it is possible to tune the degree of nonlocality

Peccianti, Conti, Assanto OL 30 , 415, 2005

The Snyder and Mitchell Science paper

Accessible Solitons

Allan W. Snyder* and D. John Mitchell

SCIENCE • VOL. 276 • 6 JUNE 1997

The refractive index perturbation is so large that the beam “samples” a small portion

$$n^2(r,P) = n_0^2 - r^2\alpha^2(P)$$

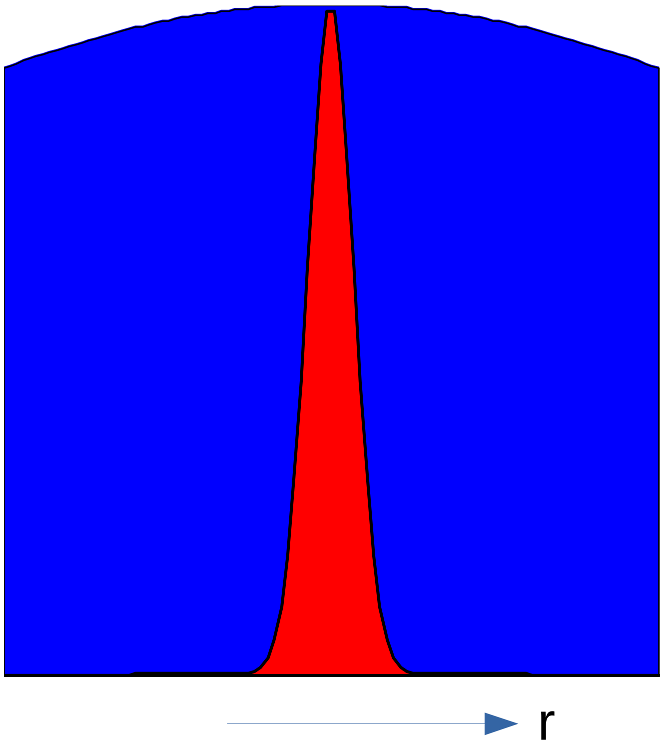

The refractive index only depens on power! Not intensity

$$2ikn_0(\partial\psi/\partial z) + \nabla_\perp^2\psi - k^2\alpha^2(P)r^2\psi = 0$$

Highly nonlocal dynamics

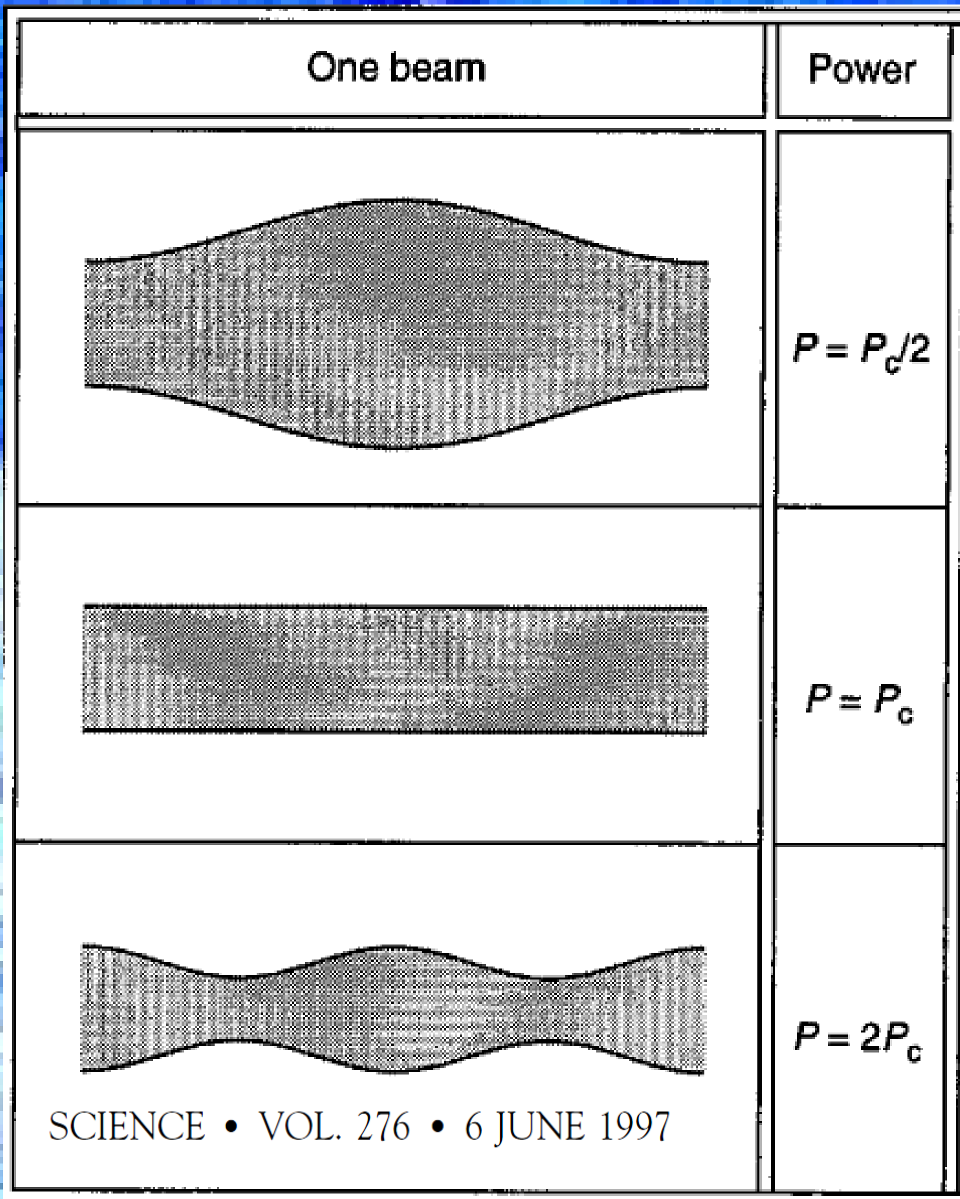

$$P w_0^4 = \text{constant}$$

Existence curve

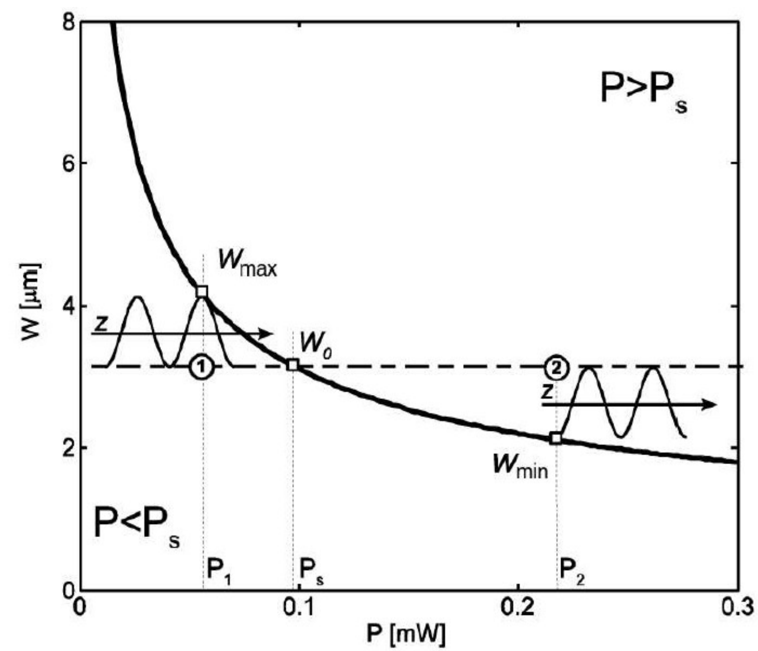

Conti et al. 92, 113 902, PRL 2004

Experimental investigations of highly nonlocal media

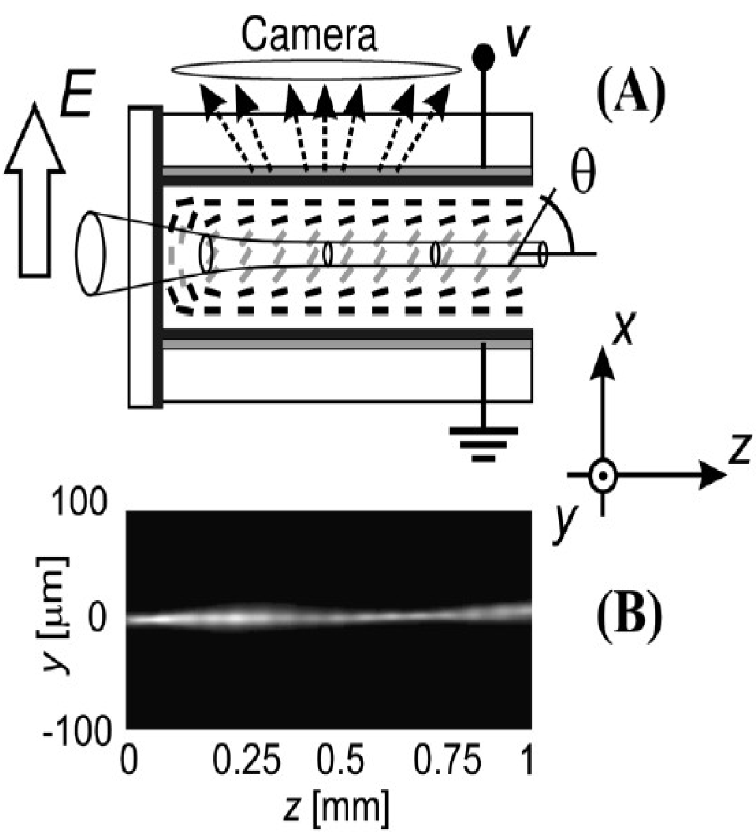

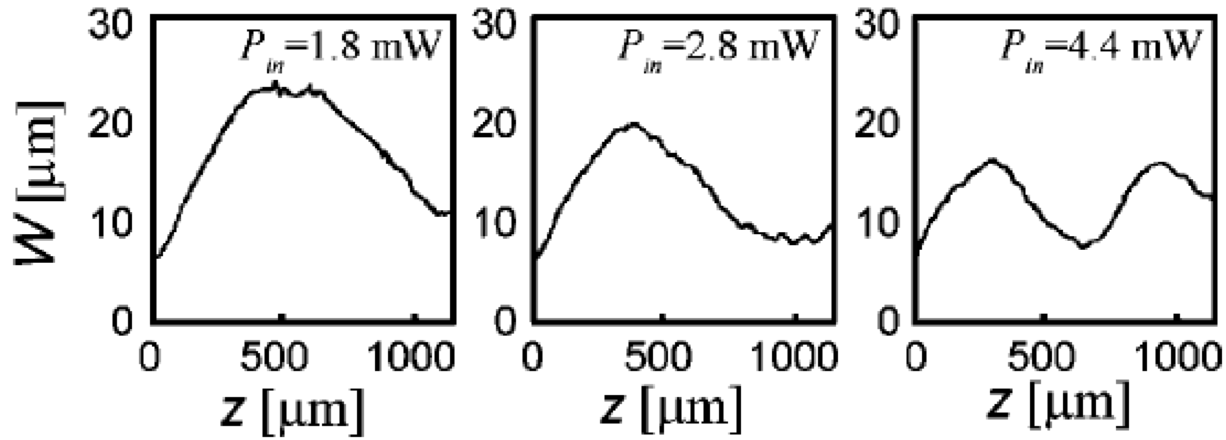

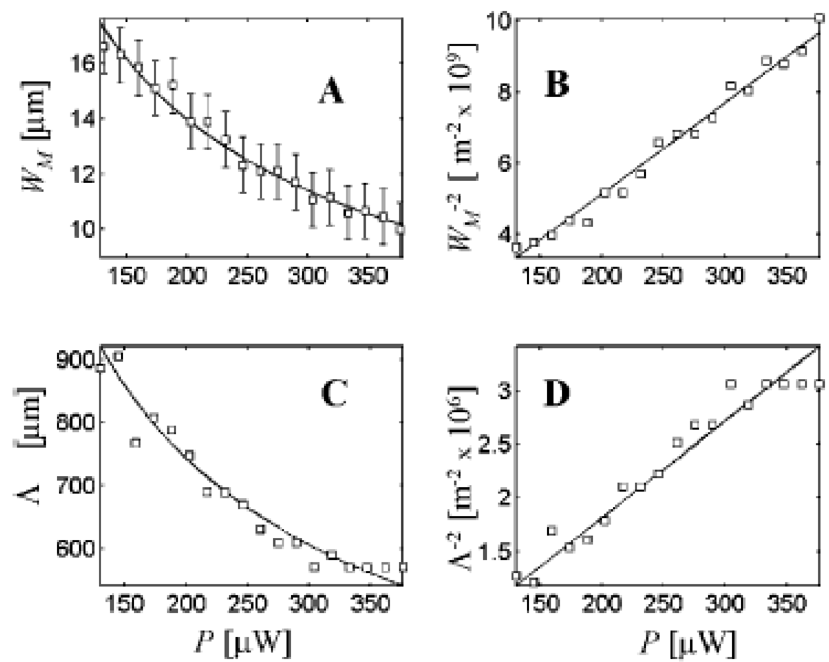

Conti et al. PRL 92, 113902, 2004

Highly and weakly nonlocal

$$2ik\frac{\partial A}{\partial z} + \nabla_\perp^2 A + \frac{2k^2}{n_0} A \int_{-\infty}^{\infty} K(x-x')I(x')dx' = 0$$

$$K(x-x') \cong K(x) \cong K_0 + K_2 x^2$$

$$P = \int I dx$$

$$2ik\frac{\partial A}{\partial z} + \nabla_\perp^2 A + \frac{2k^2}{n_0} P K(x) A = 0$$

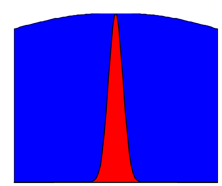

Snyder and Mitchell limit

$$S(k) = \frac{n_2}{1+\sigma^2 k_\perp^2} \cong n_2 \left(1 - \sigma^2 k_\perp^2\right)$$

$$2ik\frac{\partial A}{\partial z} + \nabla_\perp^2 A + \frac{2k^2 n_2}{n_0} \left(I + \sigma^2 \nabla_\perp^2 I\right) A = 0$$

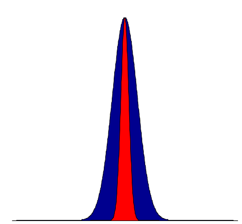

Nonlocality may also mean a dependence on the derivatives of intensity

Diffraction and spatial solitons

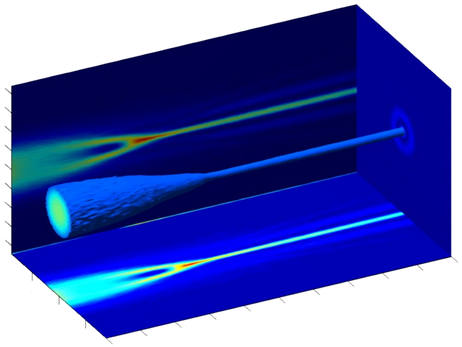

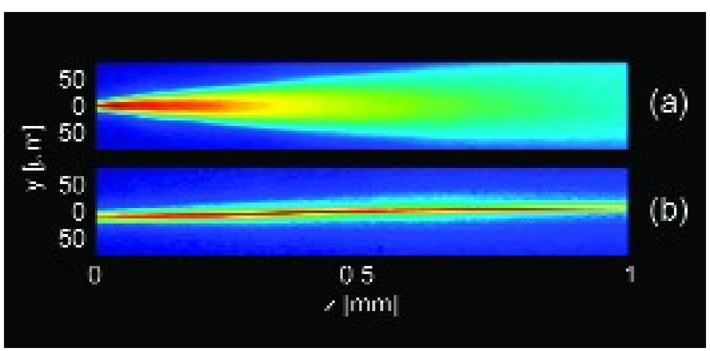

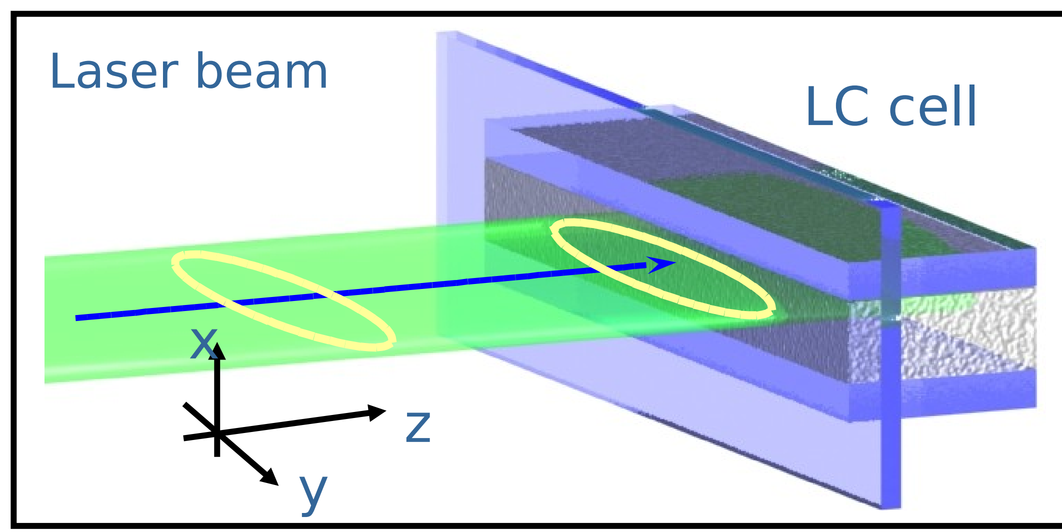

Modulational instability

- Modulation Instability:
- Exponential amplification of small perturbation

V_{bias}=1.62   λ=514.5 nm

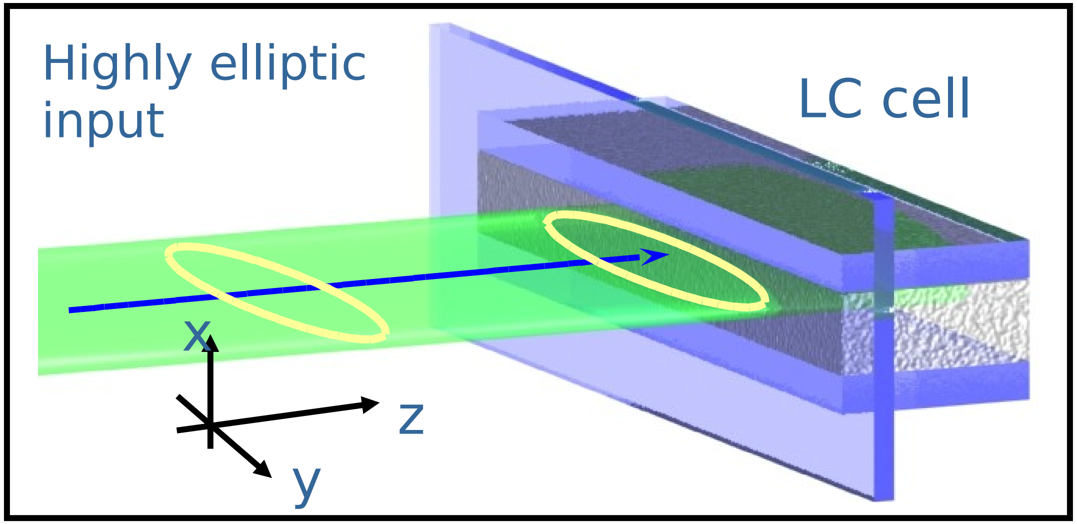

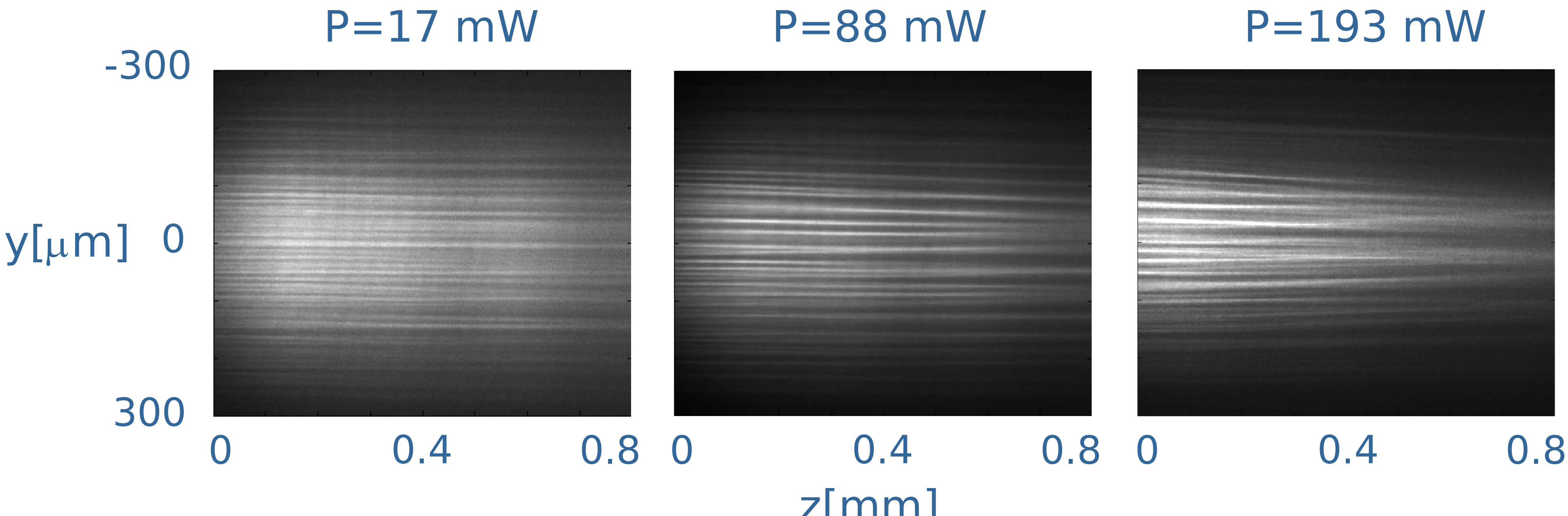

Modulational instability

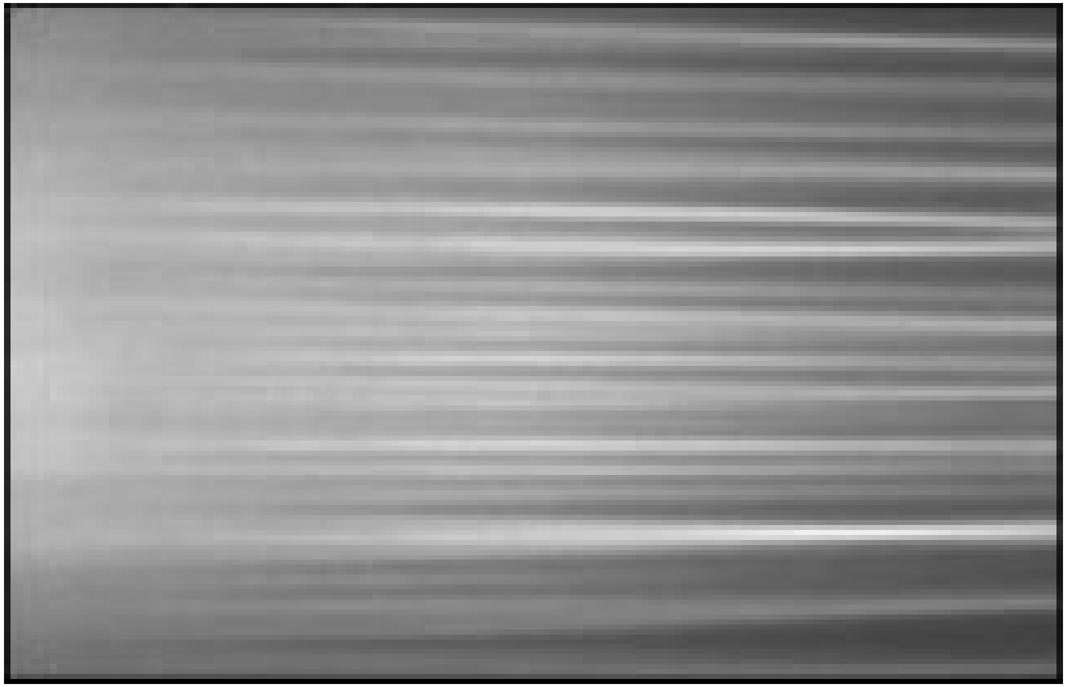

Generation of solitons that constitute the “swarm”

Geometry

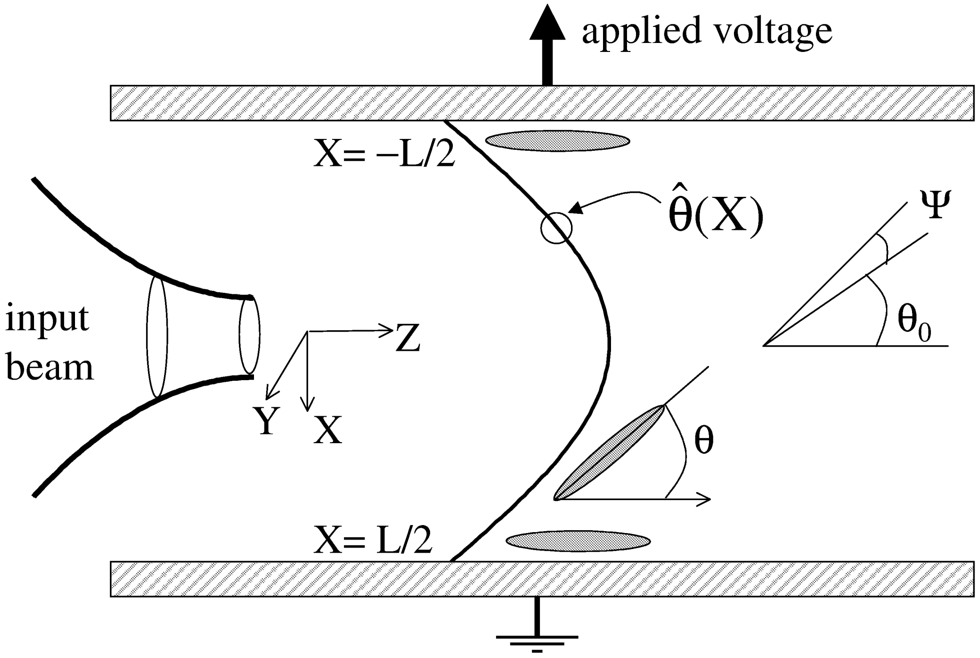

- Planar cell
- The applied voltage determines the director profile
- The optical field induces an additional (small) director tilt

$$\theta_0 \cong \frac{\pi}{4}$$ **Bulk value of the director**

$$\Psi$$ **Optical induced tilt**

Simple analysis of MI

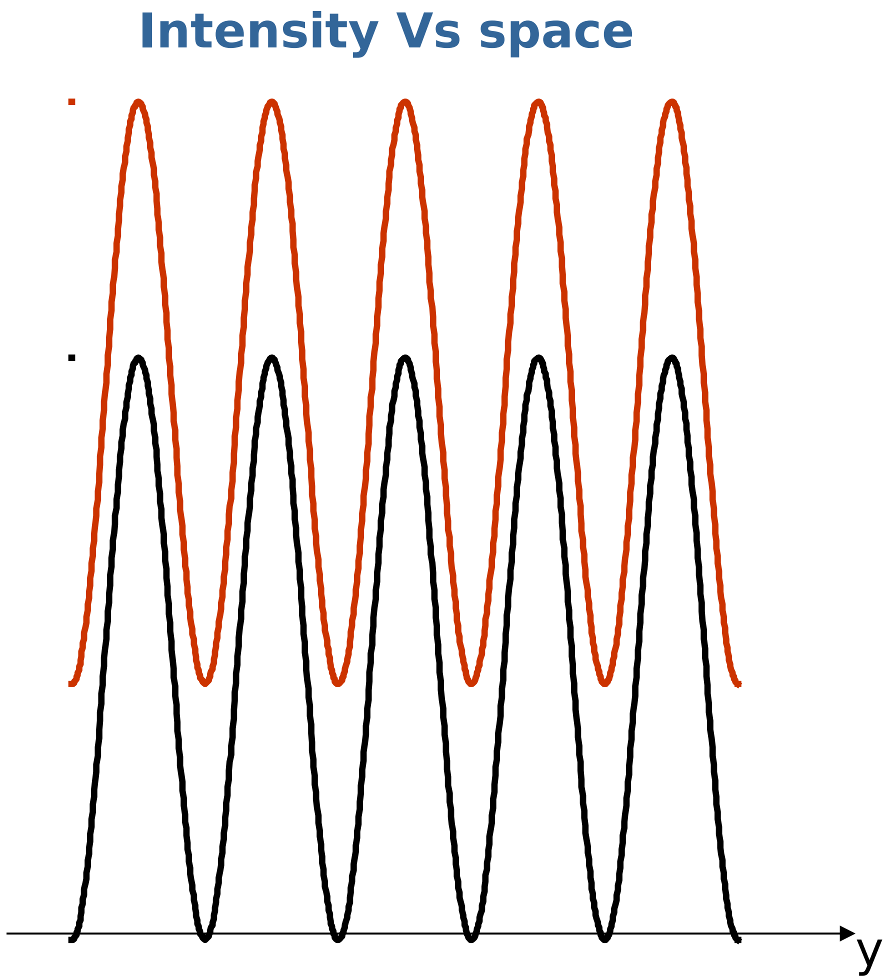

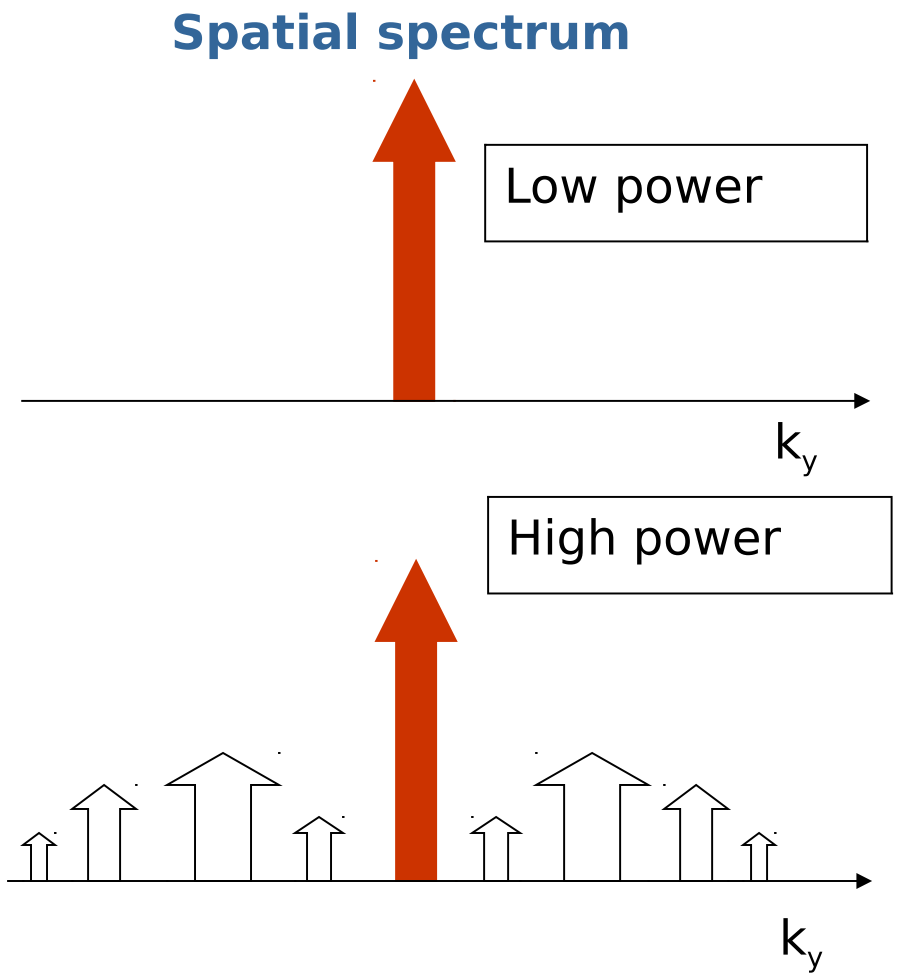

Experiments at 1.06 μm

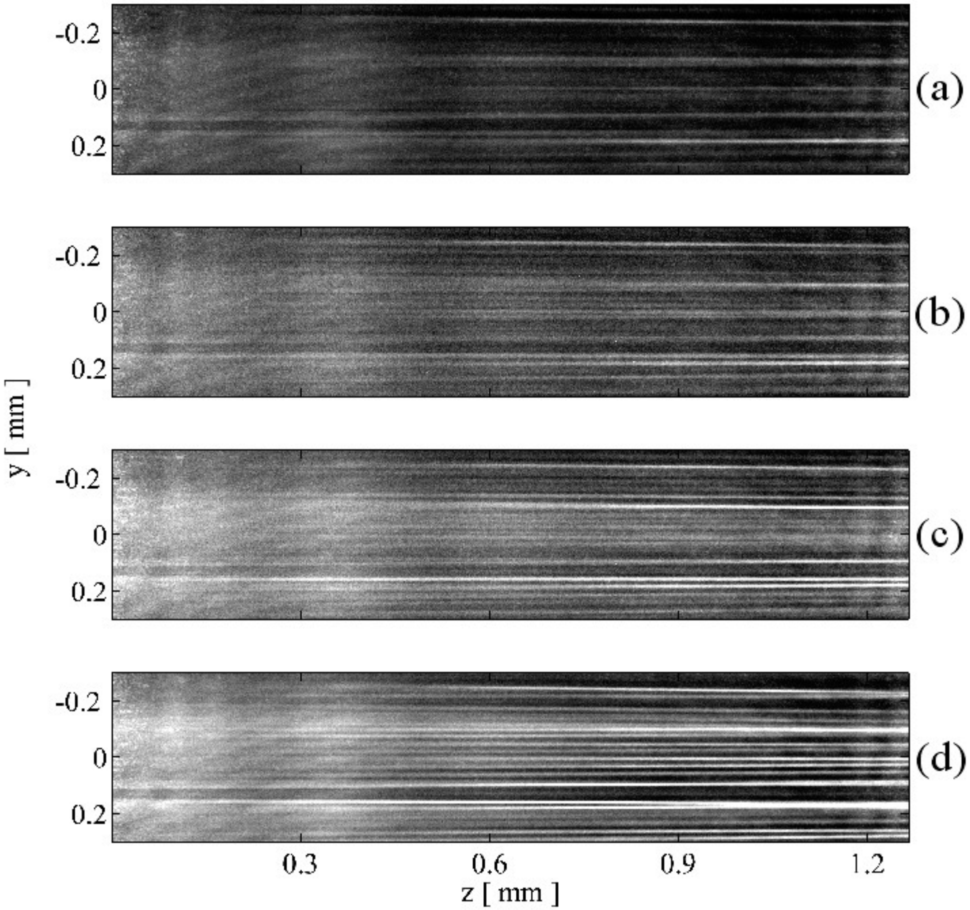

P=22mW

P=80mW

P=140mW

P=300mW

Spectrum at 1.06 μm

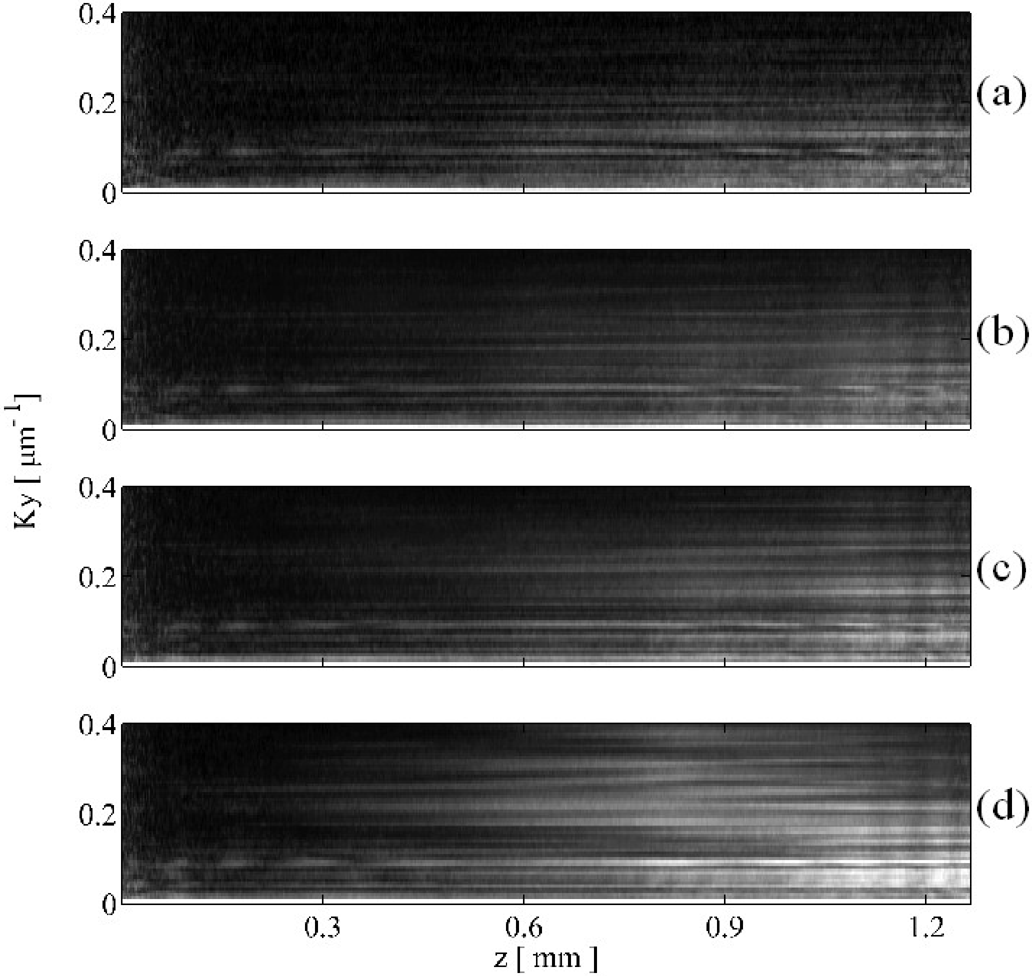

P=22mW

P=80mW

P=140mW

P=300mW

Side band modulation appears upon propagation

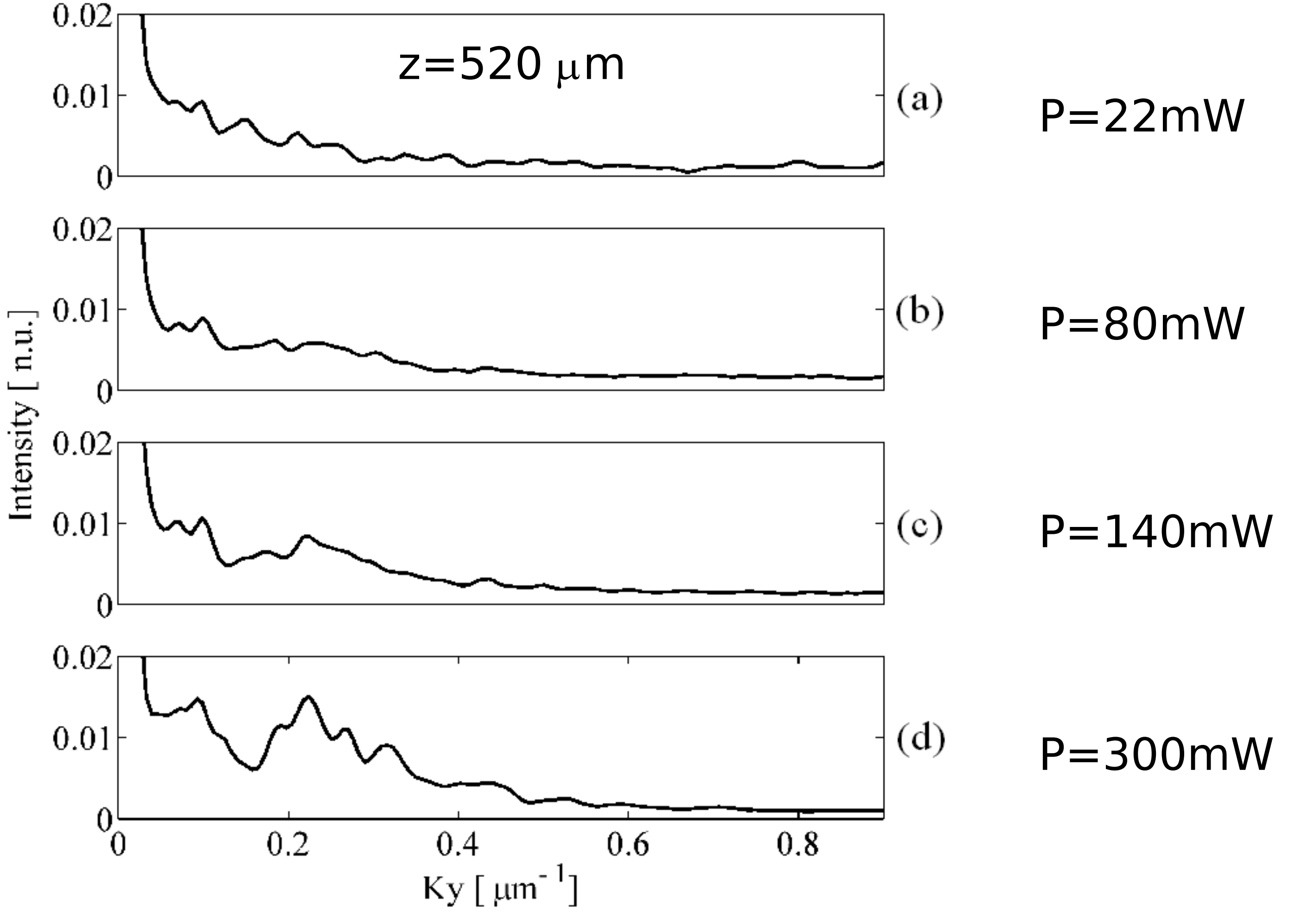

z=520 μm
P=22mW
P=80mW
P=140mW
P=300mW
(a)
(b)
(c)
(d)
Intensity [n.u.]
Ky [μm⁻¹]
0.02
0.01
0
0.2
0.4
0.6
0.8

514.5 nm

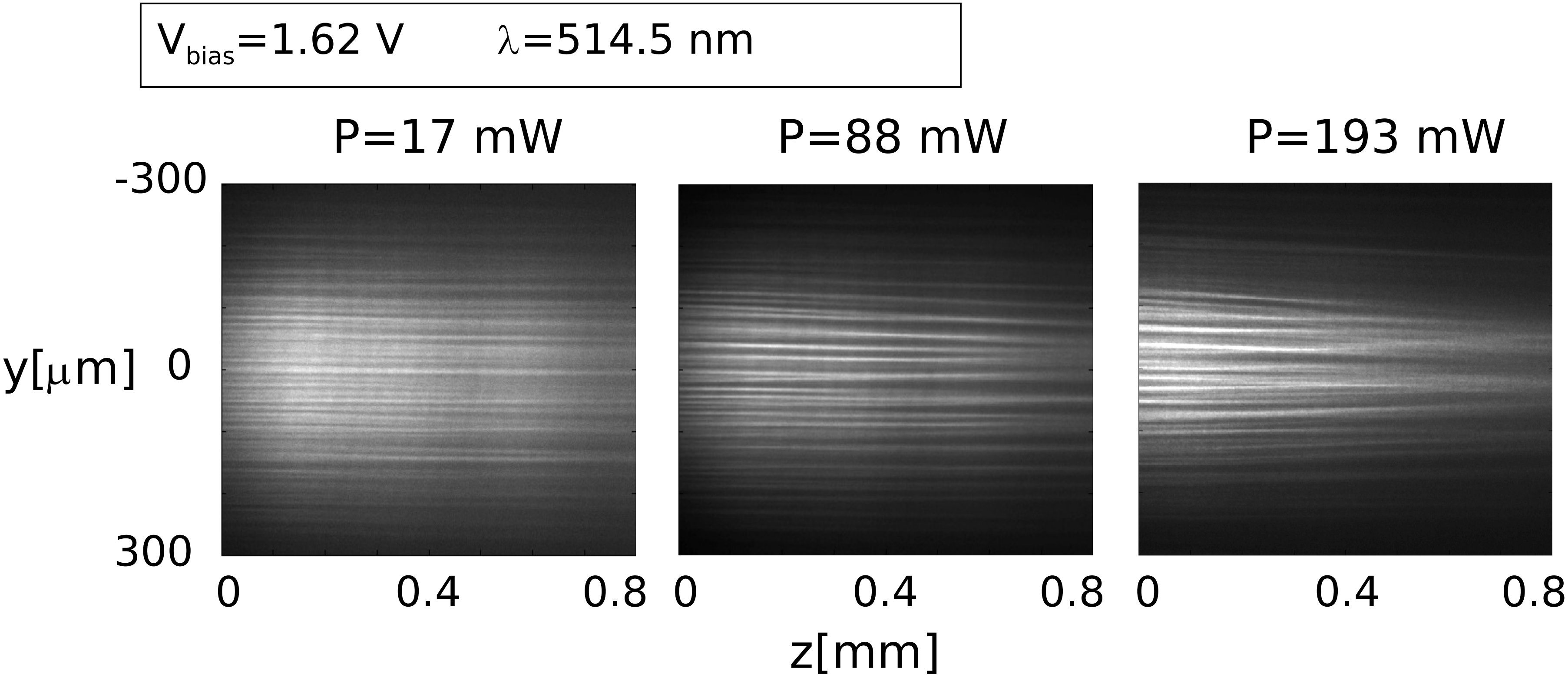

V_bias=1.62 V λ=514.5 nm
P=17 mW
P=88 mW
P=193 mW
-300
y[μm] 0
300
0
0.4
0.8
0
0.4
0.8
0
0.4
0.8
z[mm]

Experiments 514.5 nm

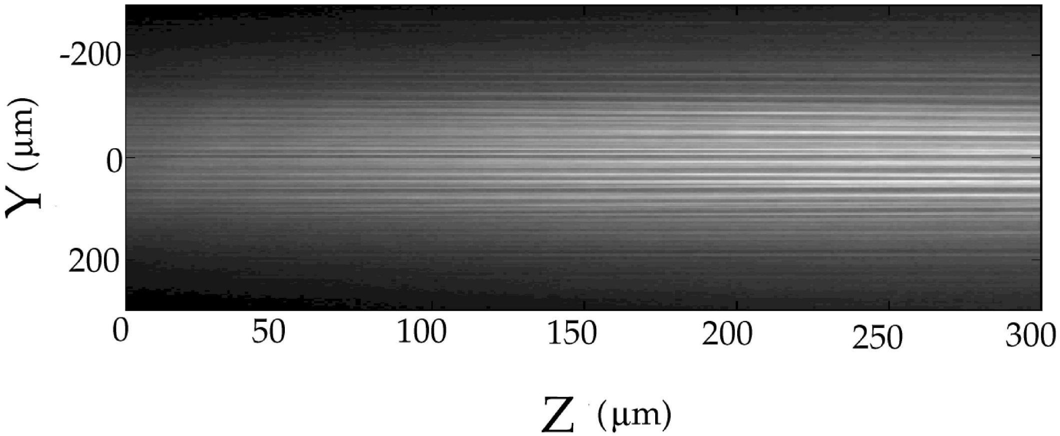

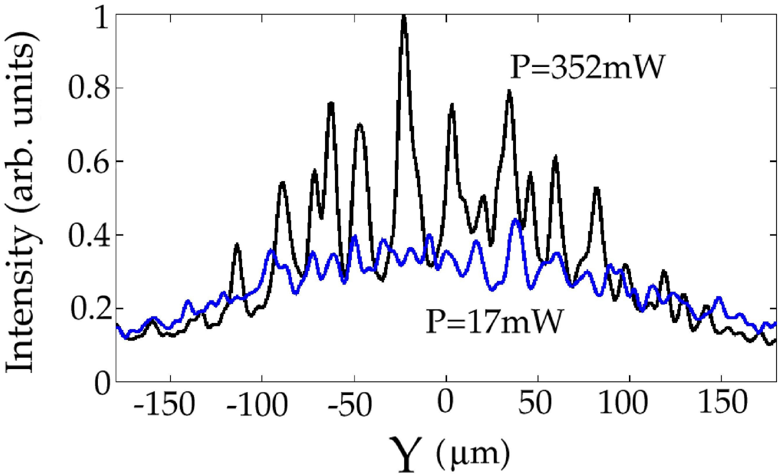

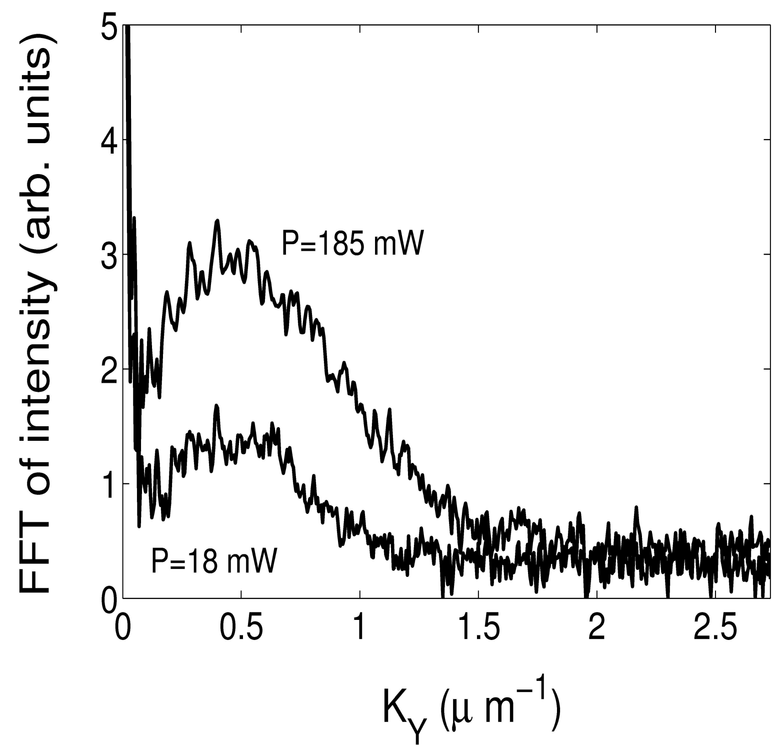

FFT of intensity (arb. units)
P=185 mW
P=18 mW
K_Y (μ m^{-1})

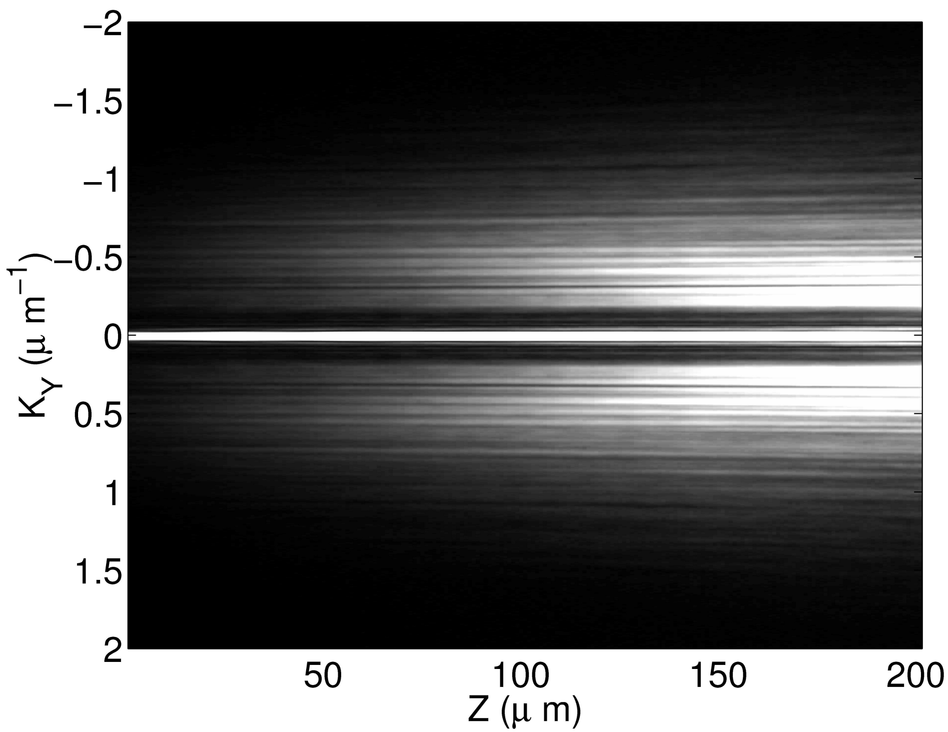

K_Y (μ m^{-1})
Z (μ m)

Theory: basic equations

Kerr medium

$$2ik\frac{\partial A}{\partial z} + \nabla_{\perp}^{2} A + 2k^{2}\frac{n_2}{n_0}|A|^{2} A = 0$$

Nematic LC (our experimental geometry)

$$2ik\frac{\partial A}{\partial z} + \nabla_{\perp}^{2} A + k_0^2 n_a^2 [\sin(\theta)^2 - \sin(\theta_0)^2]A = 0$$

$$K\frac{\partial^2\theta}{\partial z^2} + K\nabla_{\perp}^{2}\theta + \frac{\Delta\varepsilon_{RF}E^2}{2}\sin(2\theta) + \frac{\varepsilon_0 n_a^2 |A|^2}{4}\sin(2\theta) = 0$$

Theory: perturbative approach

$$\theta(x,y,z) = \theta_0 + \frac{\hat{\theta}(x)}{\theta_0}\Psi(x,y,z)$$

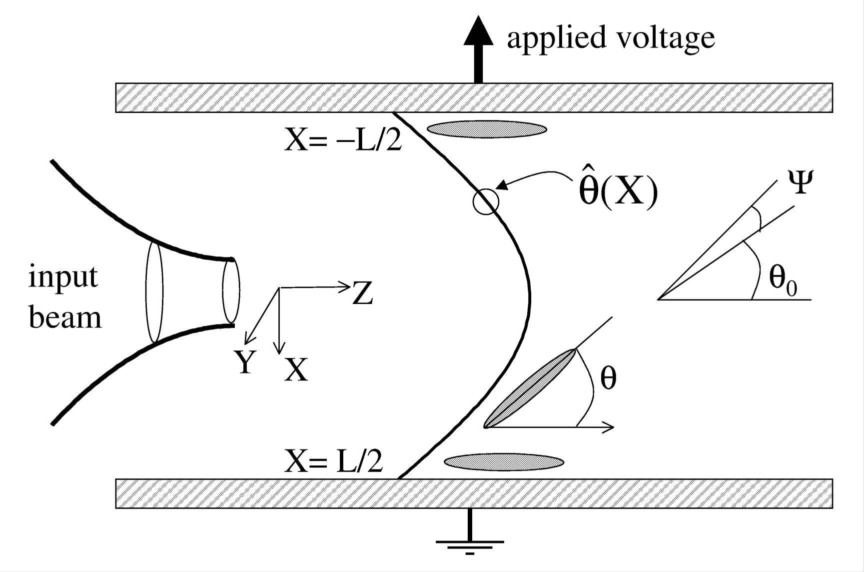

- small perturbation ($\Psi \ll \theta_0$)
- large cell (along x)
- slowly varying along z
- 1D dynamics (elliptical beam)

$$K\frac{d^2\hat{\theta}}{dx^2} + \frac{\Delta\varepsilon_{RF}E^2}{2}\sin(2\hat{\theta}) = 0$$

Resulting model

$$2ik\frac{\partial A}{\partial z}+\frac{\partial^2 A}{\partial y^2}+k_0^2 n_a^2 \Psi A=0$$

$$K\frac{\partial^2 \Psi}{\partial y^2}-\frac{2\Delta\varepsilon_{RF}E^2}{\pi}\Psi+\frac{\varepsilon_0 n_a^2}{4}|A|^2=0$$

The simplest model for a nonlocal nonlinear

- First studied by Litvak (1975) in plasma physics
- Reduced to Kerr model for K=0

Conti, Peccianti, Assanto, Phys. Rev. Lett. 91, 073901 (2003)

MI analysis

The plane wave (∂_y=0) solution is perturbed by side-band modulation

$$A = A_0 e^{i\beta_0 Z} + a_+(z) e^{ik_y y + i\beta_0 Z} + a_-(z) e^{-ik_y y + i\beta_0 Z}$$

Exact plane wave solution

The amplitudes a_+ and a_- grow exponentially for a given range of ky (MI GAIN BANDWIDTH)

MI Bandwidth 1/2

GAIN **Maximally amplified k**

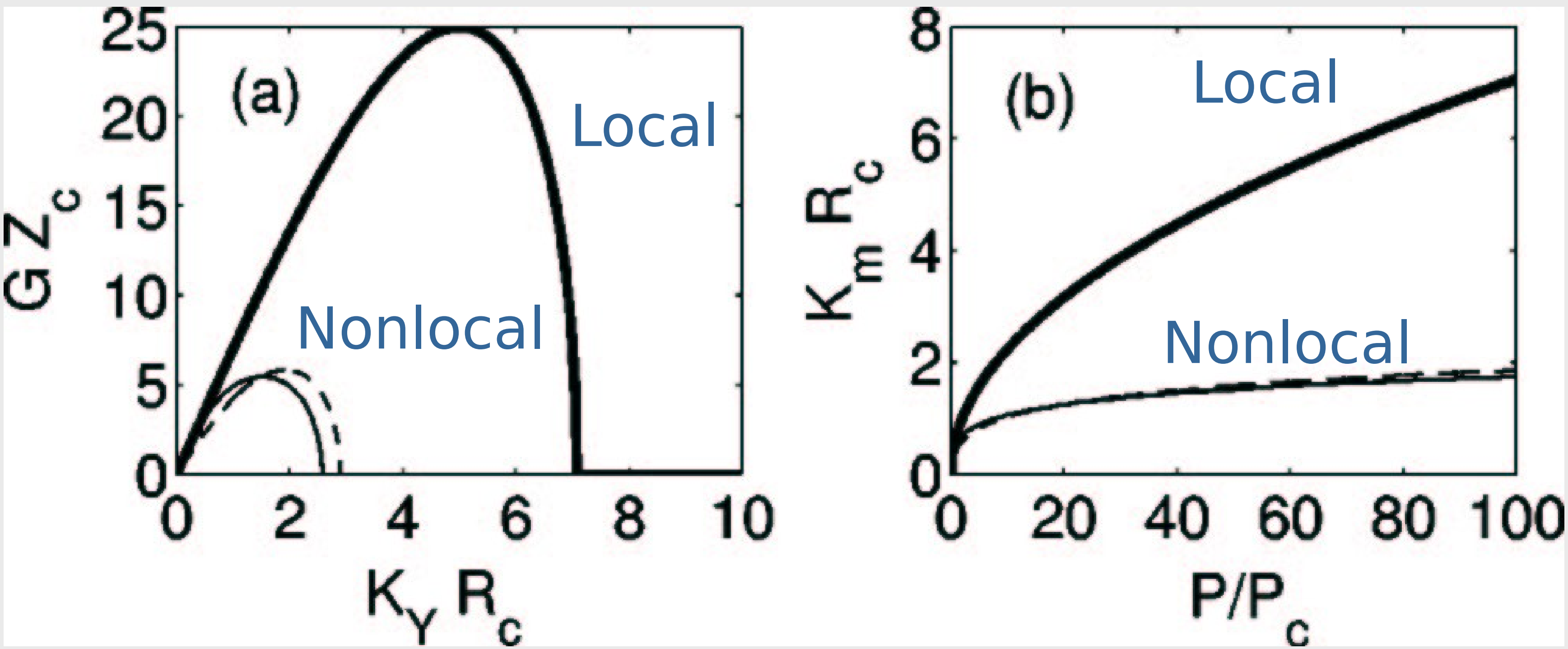

MI Bandwidth 2/2

$$G(k_y) \propto |k_y R_c| \sqrt{\frac{P}{P_{ref}} - (k_y R_c)^2}$$

"Kerr" local model

$$G(k_y) \propto |k_y R_c| \sqrt{\frac{P}{P_{ref}} \frac{1}{1+(k_y R_c)^2} - (k_y R_c)^2}$$

Additional spatial filtering

Nonlocal gain profile

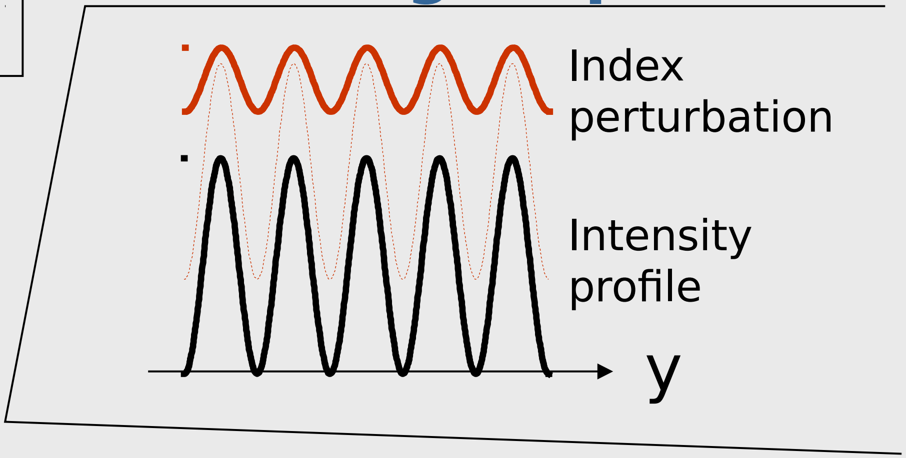

$$R_c = \sqrt{\frac{\pi K}{2\Delta\varepsilon_{RF} E^2}}$$

~Spatial filter inverse bandwidth

Quantitative analysis of MI

- The Nonlocal model works very well
- The local model overestimates of nearly two orders of magnitude

Measured maximally amplified transversal wavevector

Evidence of nonlocal MI!

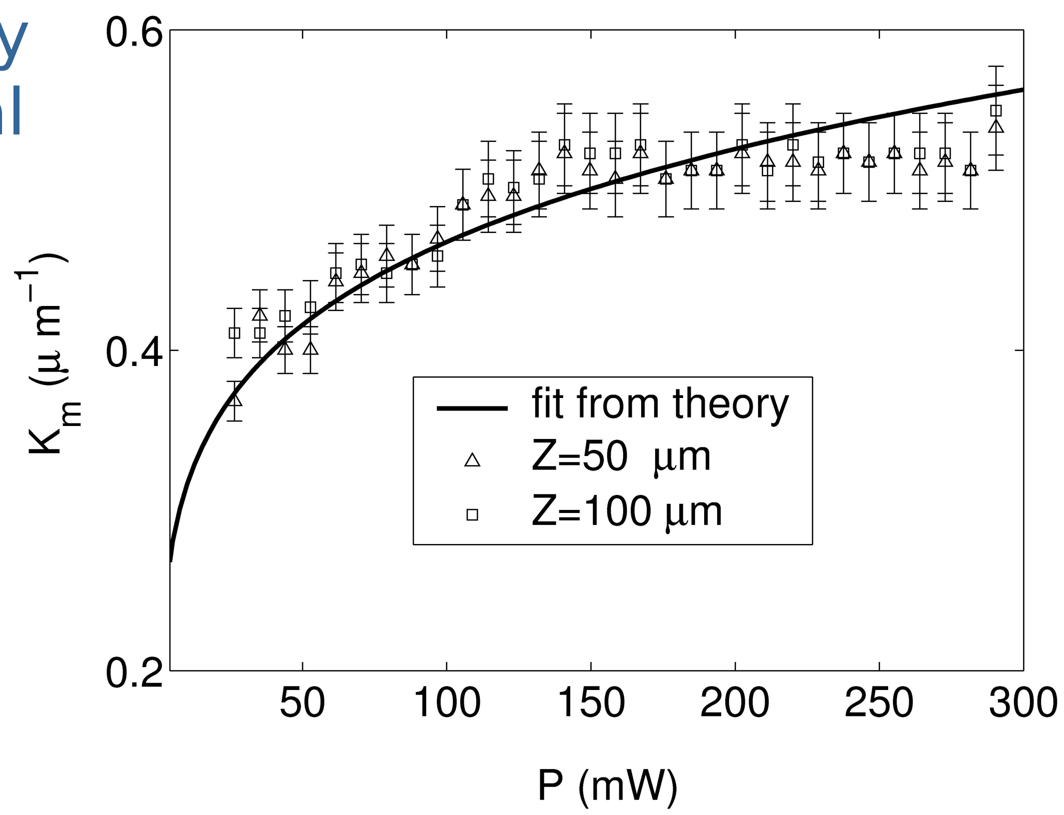

Peccianti, Conti, Assanto, Phys. Rev. E 68, 025602(R) (2003)

Summarizing

- Nonlinearity induces localization
- Localization is described by solitons
- Solitons are 1D
- Filaments are many-D
- Solitons and filaments interact
- Nowadays we make experiments with tens or hundreds of solitons

From a nonlinear wave equation to a model that resembles statistical mechanics

(simplest formulation)

Any soliton is a particle

$$2ik\frac{\partial A}{\partial z} + \frac{\partial^2 A}{\partial x^2} + 2k^2\frac{\Delta n[I]}{n}A = 0$$

$$I(x) = \sum_{p=1,N} I_p(x - x_p) \cong \sum_{p=1,N} I_S(x - x_p)$$

$$\Delta n[I] = \sum_{p=1}^{N} \Delta n[I_p].$$

CC, PRE 72, 066620 (2005)

The motion of the soliton

$$m\frac{d^2x_p}{dz^2} = -\int_{-\infty}^{\infty} I_S(x-x_p)\frac{\partial \Delta n/n}{\partial x}dx,$$

$$m = \int I_S(x)dx$$

$$\frac{\Delta n}{n} = \frac{1}{n}\sum_{q=1}^{N} \Delta n_S(x-x_q),$$

Many soliton and the landscape

$$m\frac{d^2x_p}{dz^2} = \sum_{q=1}^{N}\int_{-\infty}^{\infty} I_S(x-x_p)\frac{\partial \Delta n_S(x-x_q)/n}{\partial x}dx$$

$$= -\sum_{q=1}^{N}\int_{-\infty}^{\infty} \frac{\partial I_S}{\partial x}(x-x_p)\frac{\Delta n_S(x-x_q)}{n}dx$$

$$= \frac{\partial}{\partial x_p}\sum_{q=1}^{N}\int_{-\infty}^{\infty} I_S(x-x_p)\frac{\Delta n_S(x-x_q)}{n}dx$$

$$= -\frac{\partial}{\partial x_p}\sum_{q=1}^{N} V(x_p-x_q)$$

$$V(x) = -\frac{1}{n}\int_{-\infty}^{\infty} \Delta n_S\left(\xi+\frac{x}{2}\right) I_S\left(\xi-\frac{x}{2}\right)d\xi$$

Pairwise potential

$$m\frac{d^2x_p}{dz^2} = -\frac{\partial\Phi}{\partial x_p}$$

$$\Phi = \frac{1}{2}\sum_{j=1}^{N}\sum_{k=1}^{N} V(x_j - x_k)\,.$$

$$m\frac{d^2x_p}{dz^2} = -\frac{\partial\Phi}{\partial x_p} + \eta_p(z)\,.$$

$$\langle \eta_p(z)\,\eta_q(z')\rangle = S_p^2\delta_{pq}\delta(z - z')$$

Gaussian attractive potential

$$I_S(x) = I_0 \exp\left(-\frac{x^2}{2w^2}\right),$$

$$\Delta n_S(x) = \Delta n_0 \exp\left(-\frac{x^2}{2v^2}\right)$$

$$V(x) = -\frac{1}{n}\int_{-\infty}^{\infty} \Delta n_S\left(\xi + \frac{x}{2}\right) I_S\left(\xi - \frac{x}{2}\right) d\xi$$

$$V(x) = V_0\left[1 - \exp\left(-\frac{x^2}{2u^2}\right)\right]$$

$V_0 = \Delta n_0 I_0 [2\pi v^2 w^2/(v^2+w^2)]^{1/2}$ and $u^2 = v^2 + w^2$

Particle trajectories 1/2

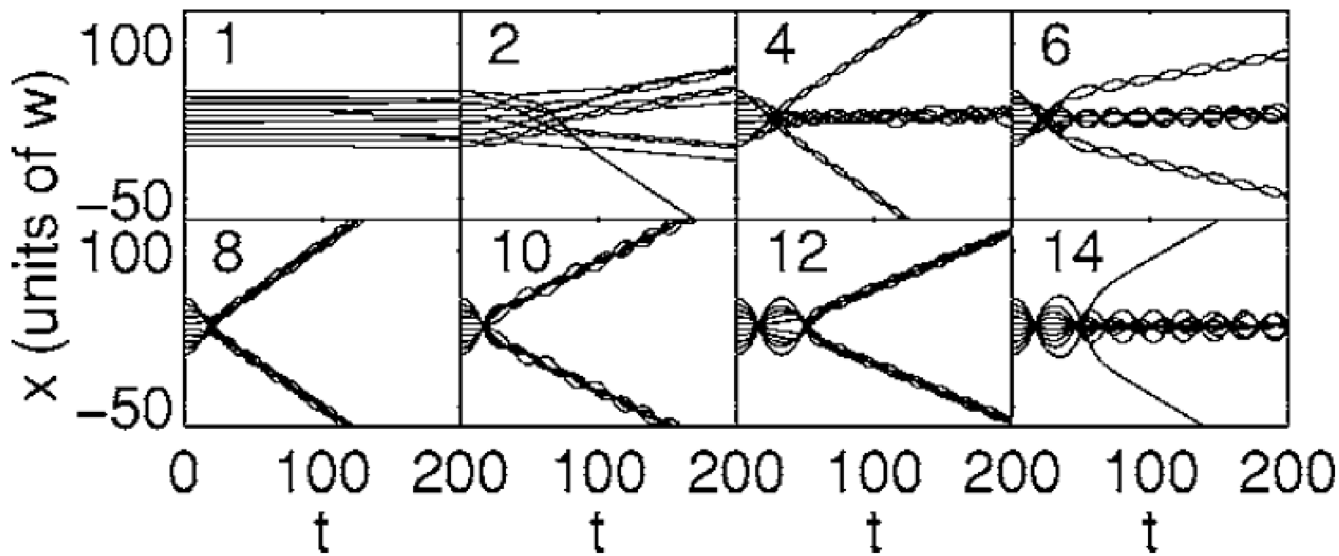

FIG. 1. Filaments trajectories vs the normalized propagation coordinate t for a given noise realization and various values of the interaction range u/w (here $N=10$).

Particle trajectories 1/2

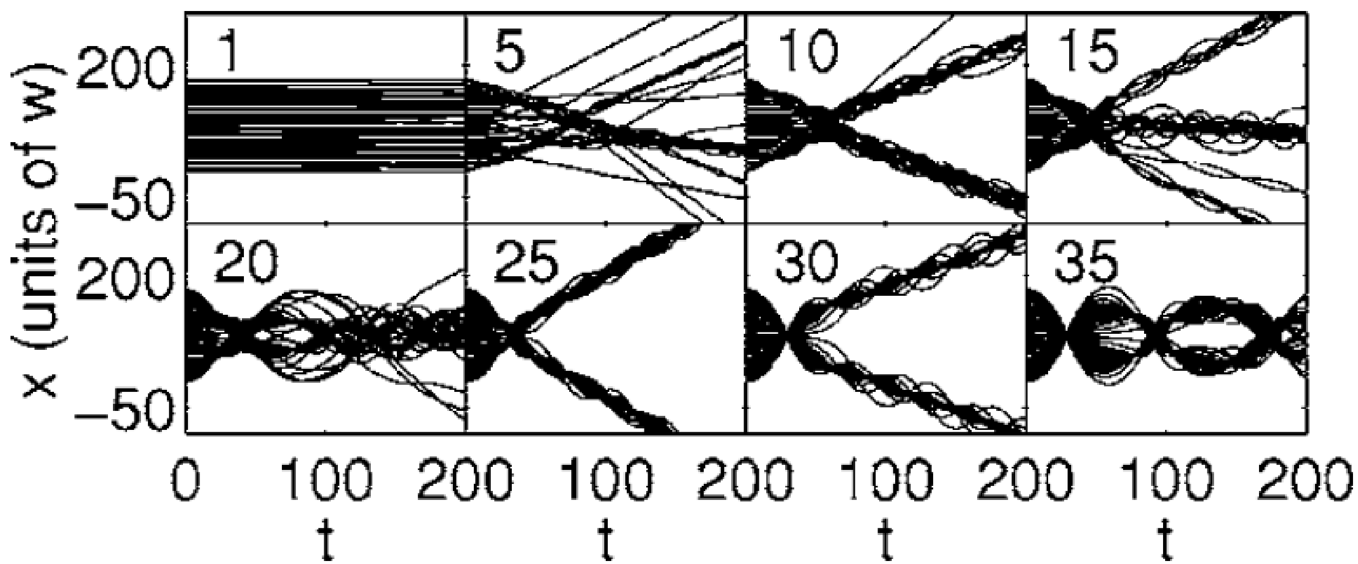

FIG. 2. Filaments trajectories vs the normalized propagation coordinate t for a given noise realization and various values of the interaction range u/w (here $N=30$).

Final positions varying noise 1/2

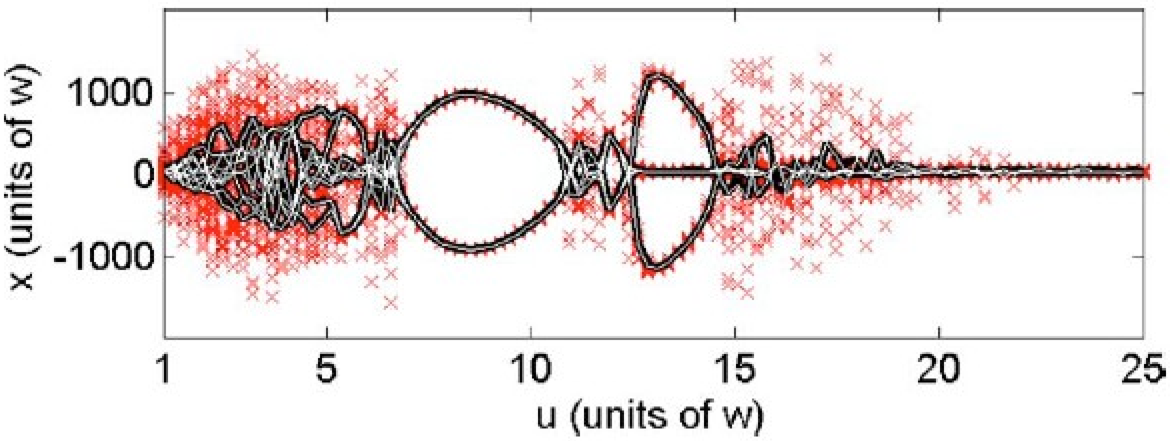

FIG. 3. (Color online) Crosses, filament positions at $t_{max} = 1000$ for ten noise realizations; thick black line, average position (see text); and white line, inherent structures (here $N = 10$).

Final positions varying noise 2/2

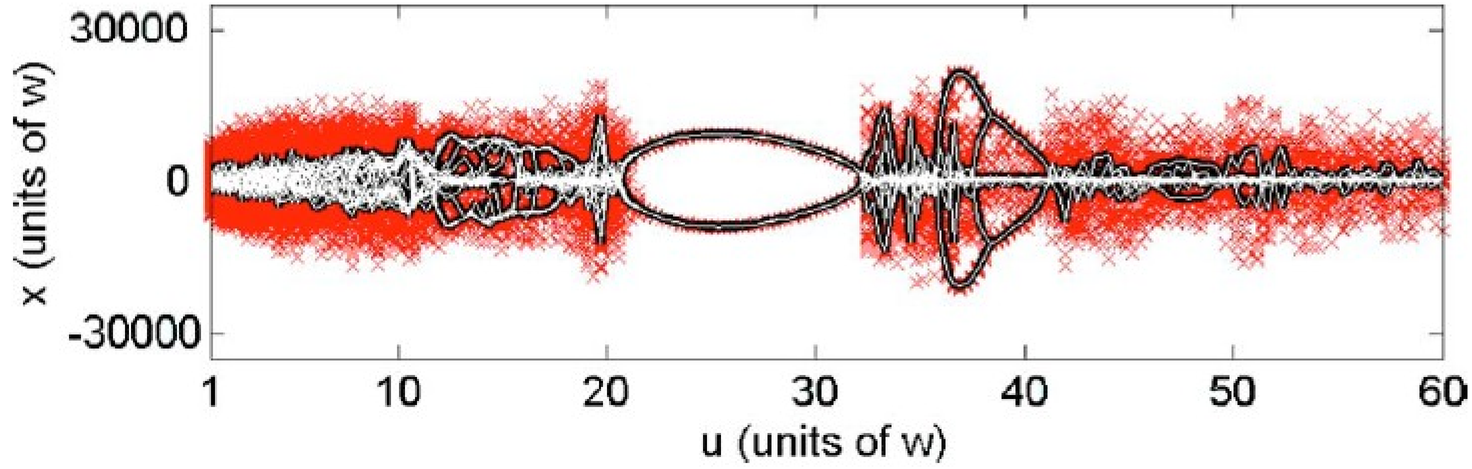

FIG. 4. (Color online) Crosses, filament positions at $t_{max} = 6000$ for ten noise realizations; thick black line, average position (see text); and white line, inherent structures (here $N = 30$).

The inherent structure 1/2

The nearest minimum of the potential after a long propagation

Its energy unveils specific dynamic phases Vs interaction length

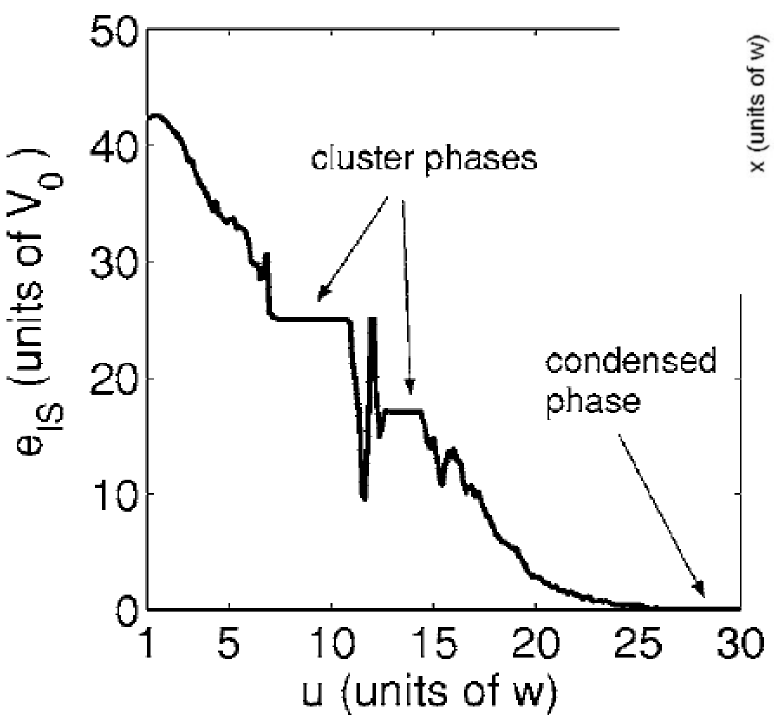

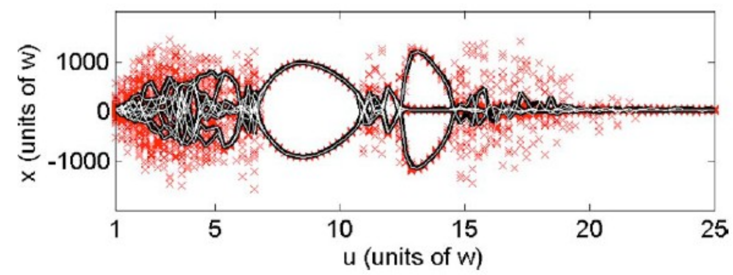

FIG. 5. Average potential energy Φ of the inherent structure e_{IS} in units of V_0 vs u/w; 1000 noise realizations have been considered $(N=10)$.

The inherent structure 2/2

The nearest minimum of the potential after a long propagation

Its energy unveils specific dynamic phases Vs interaction length

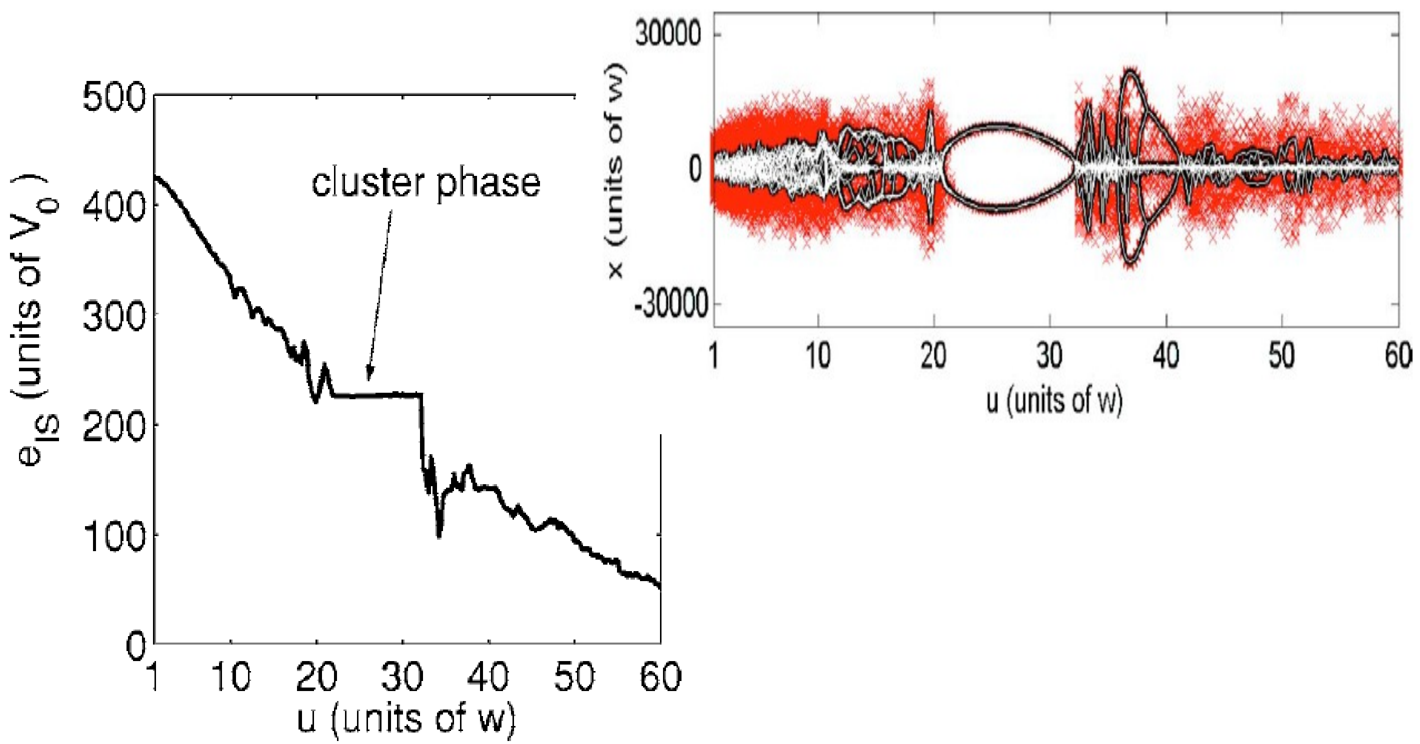

FIG. 6. Average potential energy Φ of the inherent structure e_{IS} in units of V_0 vs u/w; 100 noise realizations have been considered ($N=30$).

The generalized inherent structure

The nearest saddle point to the long time configuration

Its order (number of negative eigenvalues) has a minimum at the dynamic phase transition

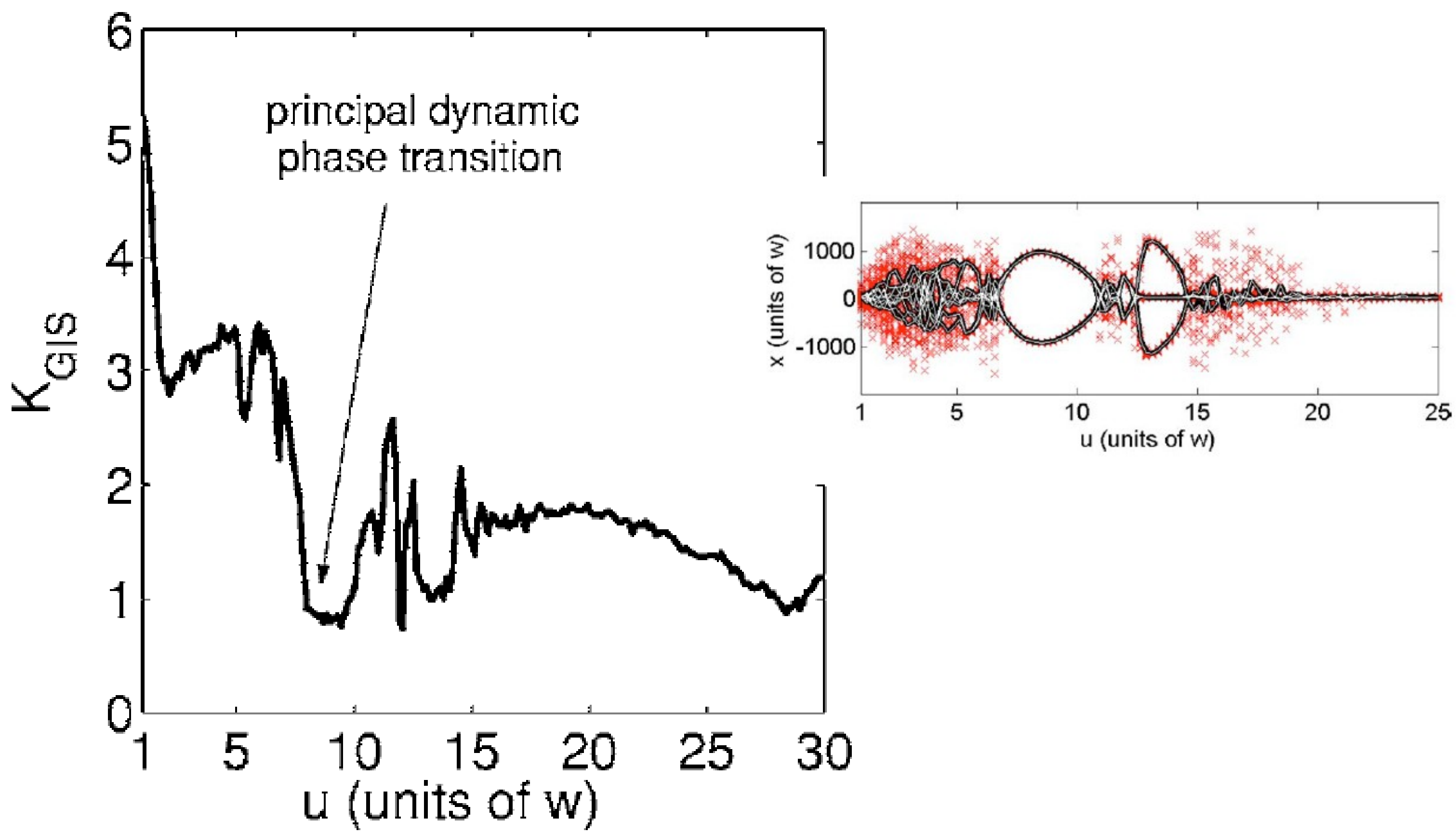

FIG. 7. Average saddle-order for the case $N = 10$, other parameters as in Fig. 5.

The generalized inherent structure

The nearest saddle point to the long time configuration

Its order (number of negative eigenvalues) has a minimum at the dynamic phase transition

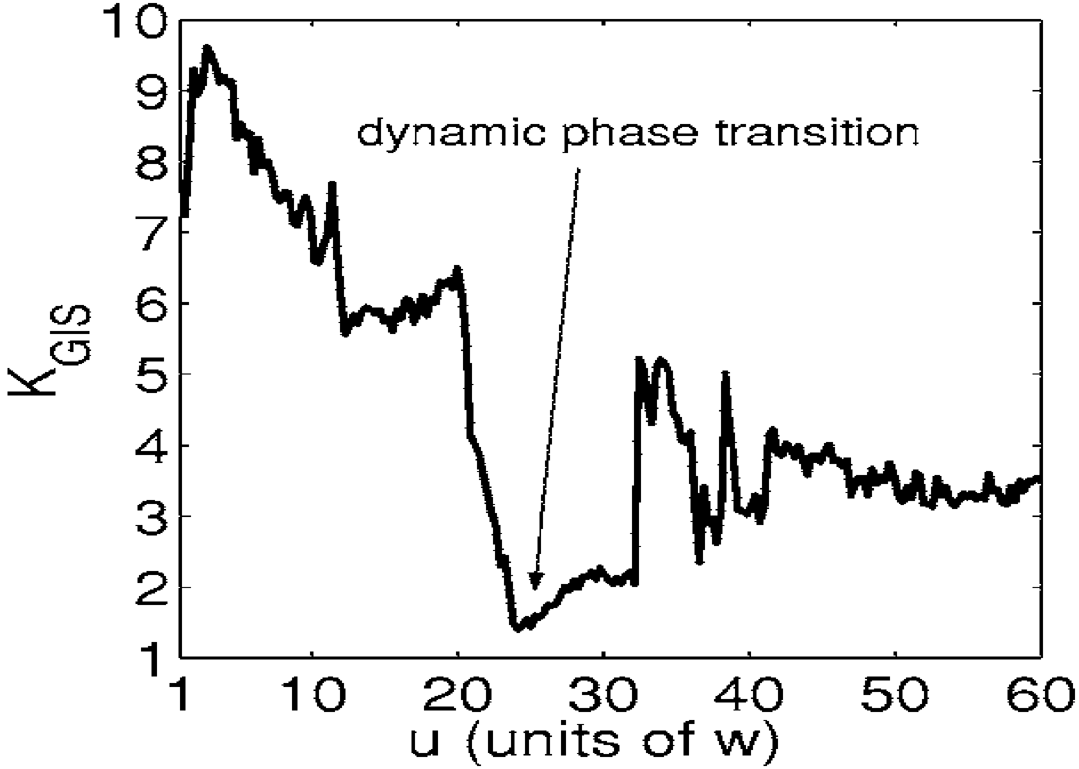

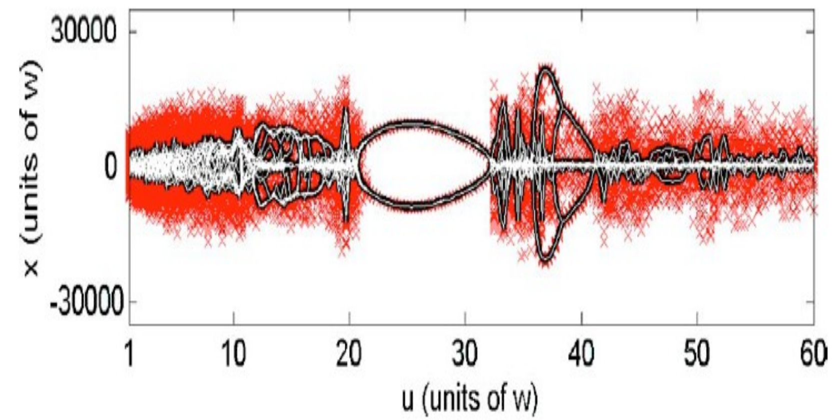

Are these features present in the wave?

We want to test the link between the particle trajectories and the wave-function

$$i\partial_{\zeta}\psi + \partial_{\xi\xi}\psi + \rho\psi = 0,$$

$$-\sigma^2\partial_{\xi\xi}\rho + \rho = |\psi|^2 + A\,\eta(\xi,\zeta)\,.$$

Wave-equation (sims)

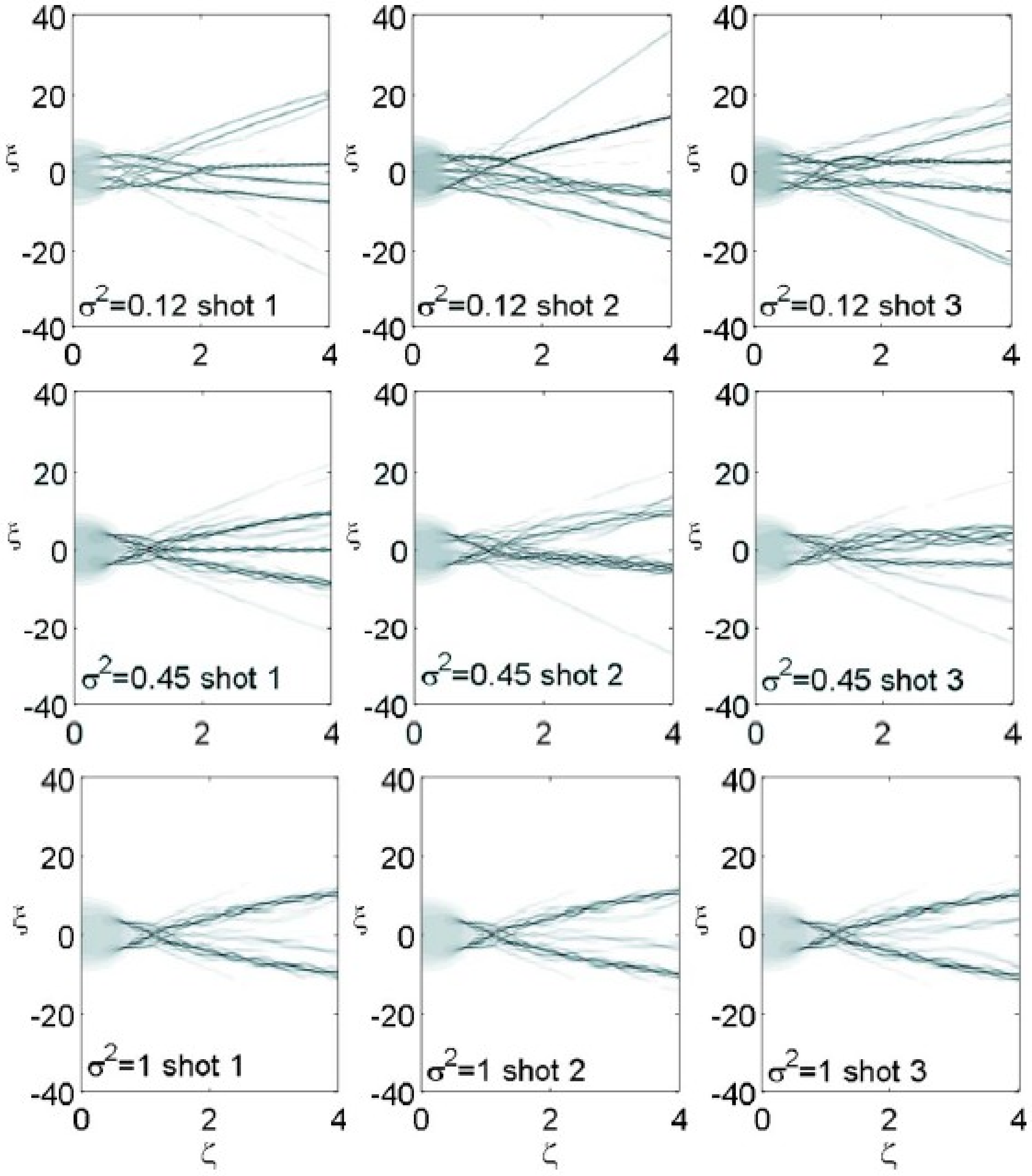

Final wave profile

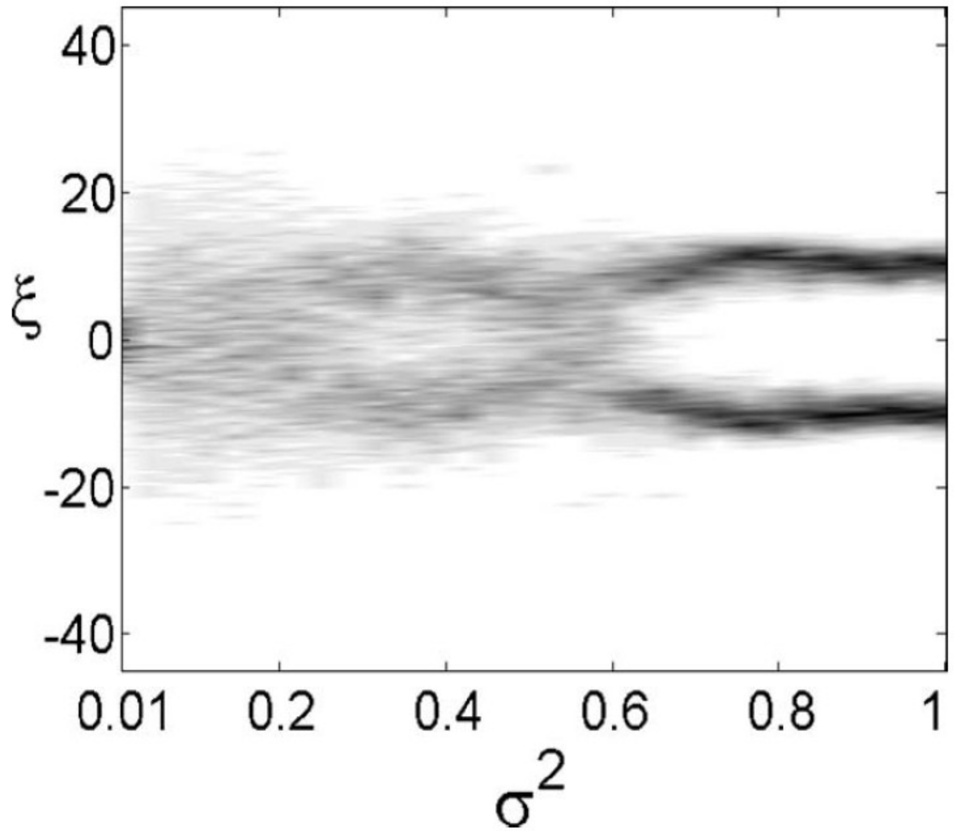

FIG. 18. Average intensity distribution at $\zeta=4$ over 100 noise realizations as a function of ξ and σ^2.

Experiments

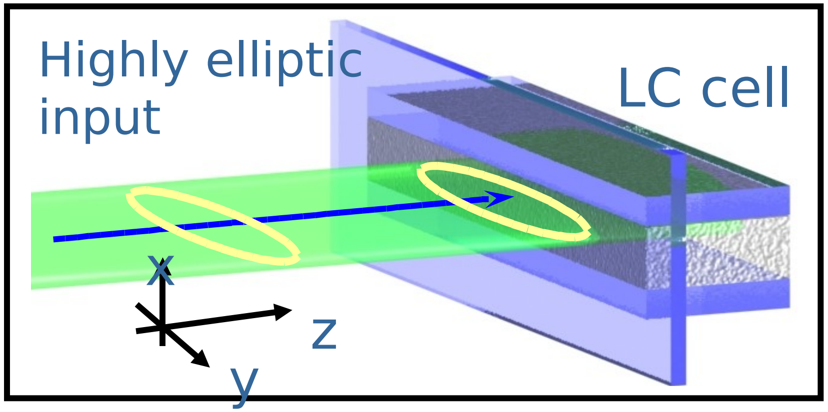

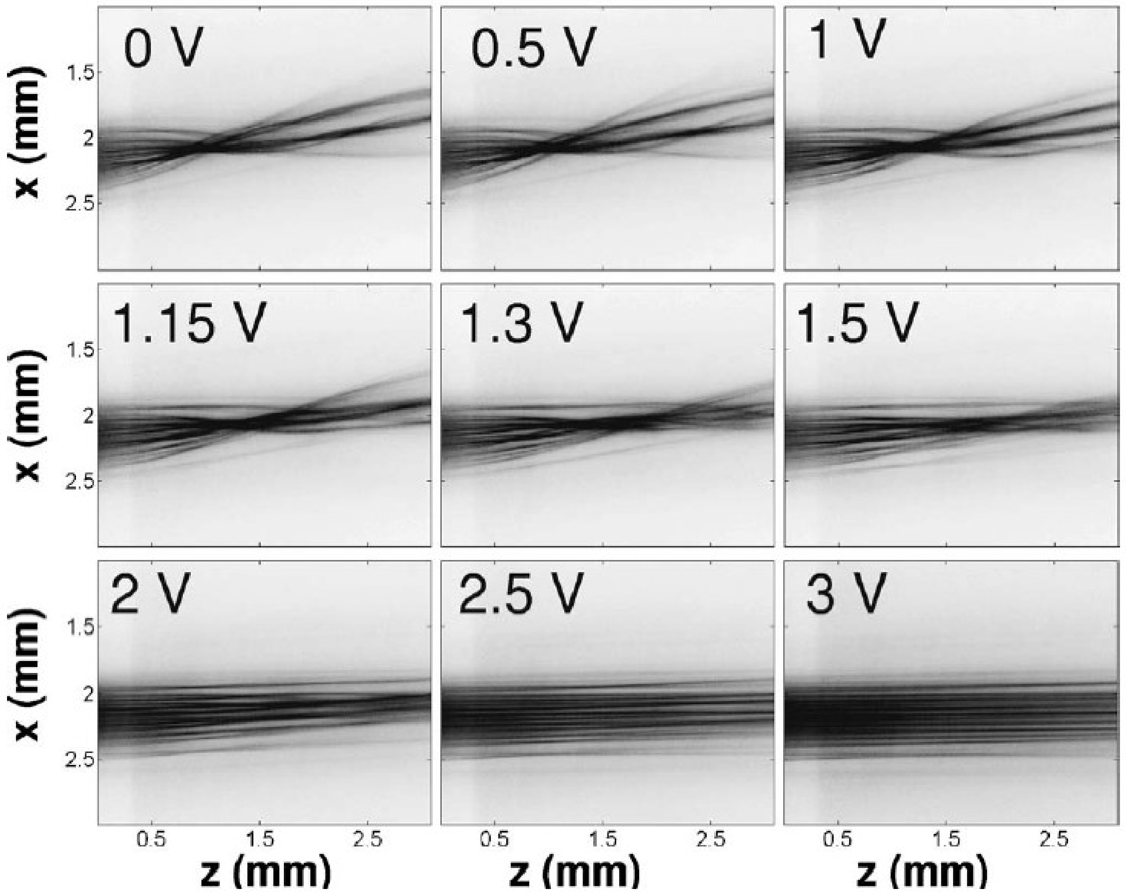

Experiments

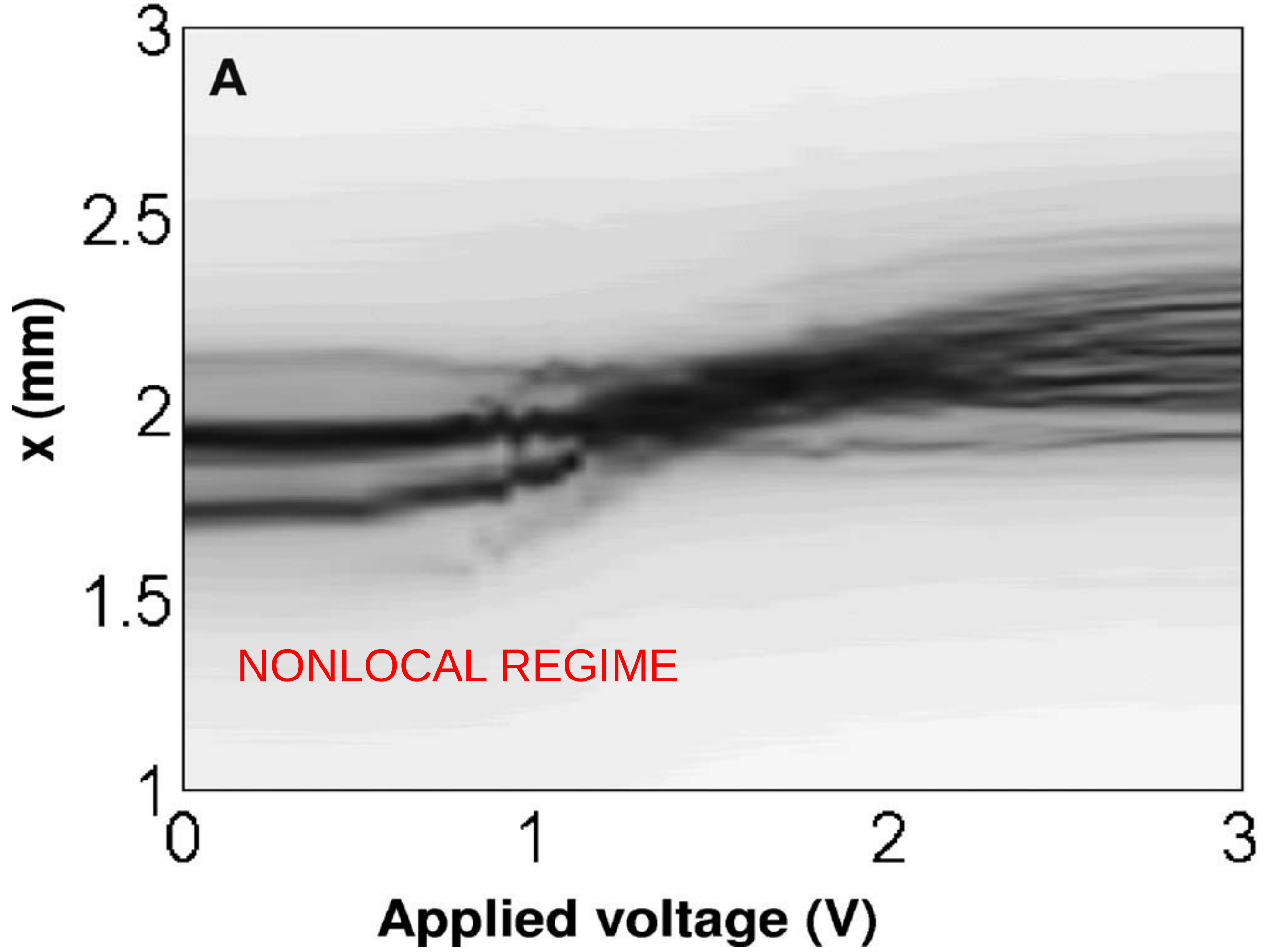

Rogue waves

or

Rogue solitons

Experiments reveal that these instabilities yield long-tailed statistics

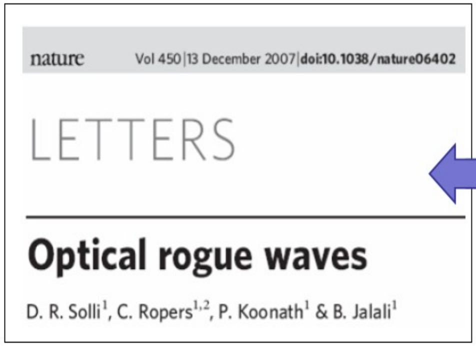
nature Vol 450|13 December 2007|doi:10.1038/nature06402

LETTERS

Optical rogue waves

D. R. Solli[1], C. Ropers[1,2], P. Koonath[1] & B. Jalali[1]

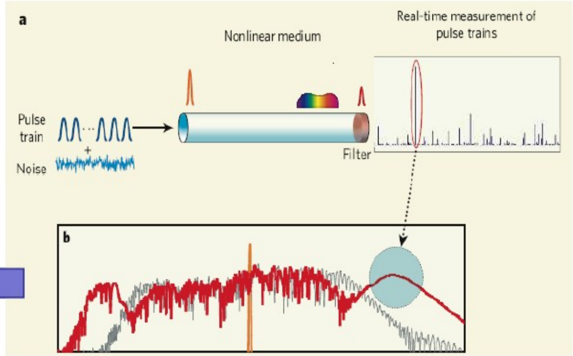

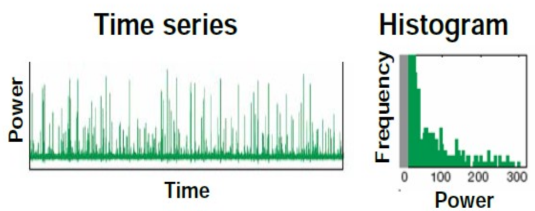

Potential Energy Landscape

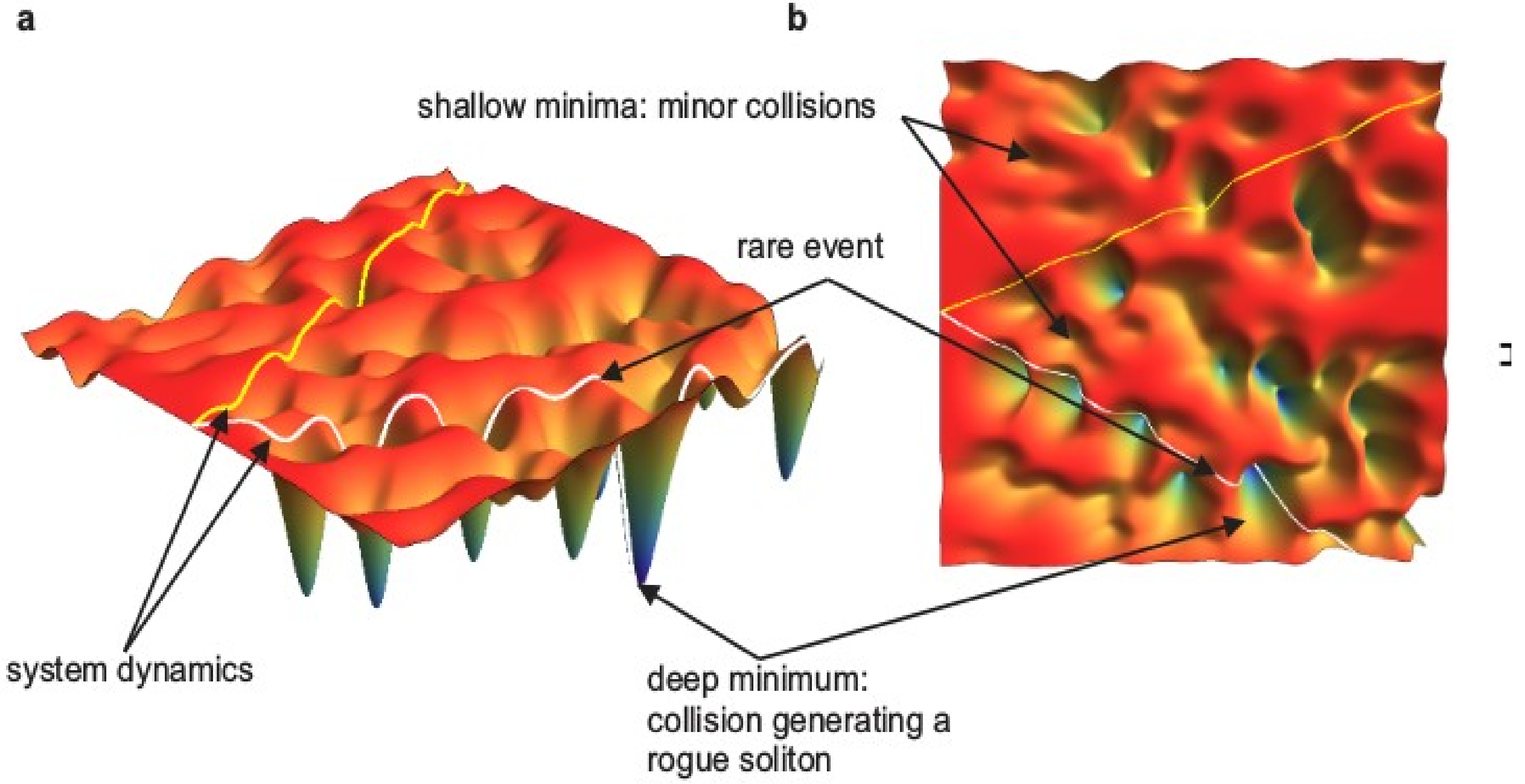

A link between the statistics of rogue waves and the statistics of minima?

Temporal Soliton

We consider a regime in which the spatial shape is constant

We consider a pulse propagating in a fiber

The pulse obeys again the NLS but with time instead of space

Filaments are replaced by light pulses

$$\frac{\partial A}{\partial z} + \frac{\alpha}{2}A - \sum_{k\geq 2}\frac{\mathrm{i}^{k+1}}{k!}\beta_k\frac{\partial^k A}{\partial T^k} = i\gamma\left(1 + \mathrm{i}\tau_{\mathrm{shock}}\frac{\partial}{\partial T}\right)\left(A(z,t)\int_{-\infty}^{+\infty}R(T')|A(z,T-T')|^2 dT'\right)$$

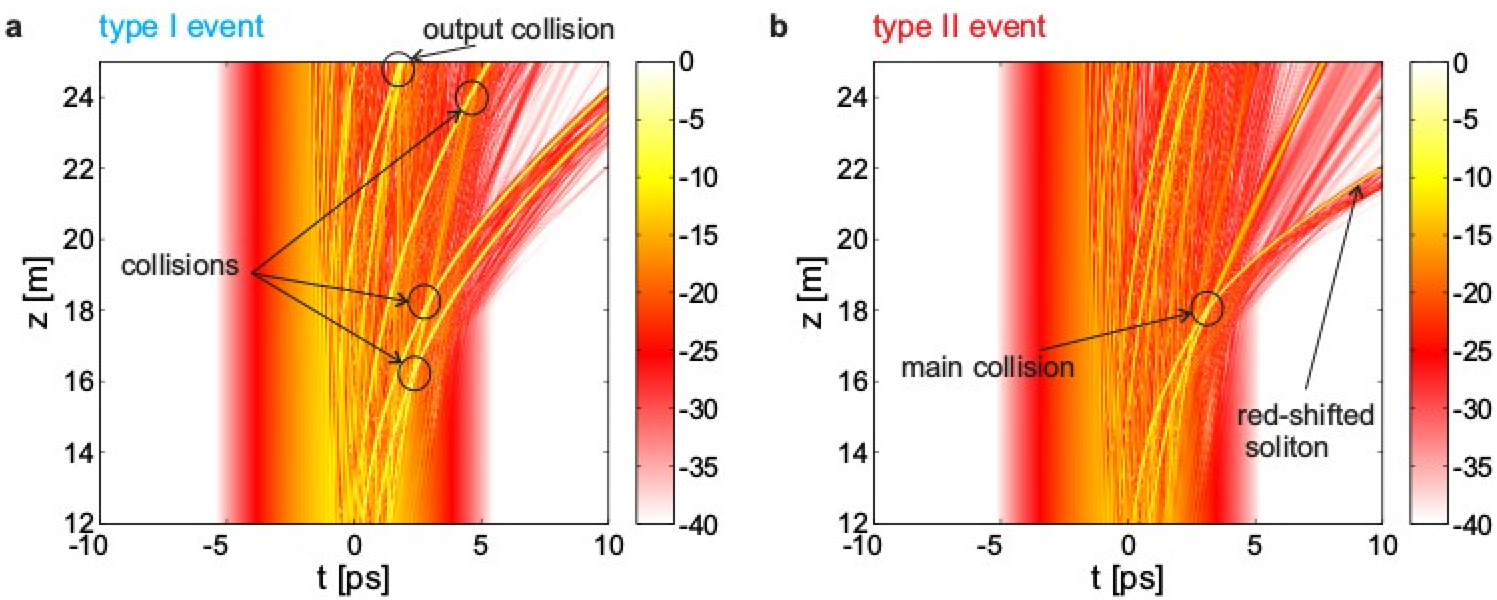

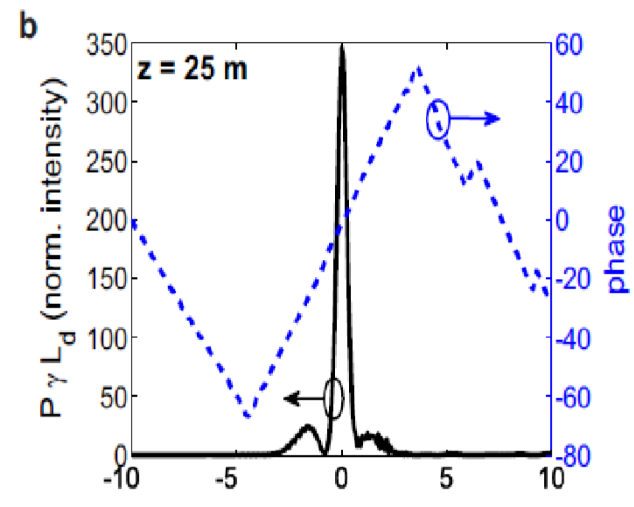

Linear waves and dispersion

$$i\frac{\partial u}{\partial z} + \frac{1}{2}\frac{\partial^2 u}{\partial t^2} + |u|^2 u = 0,$$

$$i\frac{\partial U}{\partial Z} + \sum_{k\geq 2}\frac{i^k}{k!}\beta_k\frac{\partial^k U}{\partial T^k}$$
$$+\gamma\left(1 + i\tau_{\text{shock}}\frac{\partial}{\partial T}\right)U\int_0^\infty R(T')|U(T-T')|^2\mathrm{d}T' = 0$$

Tens of solitons

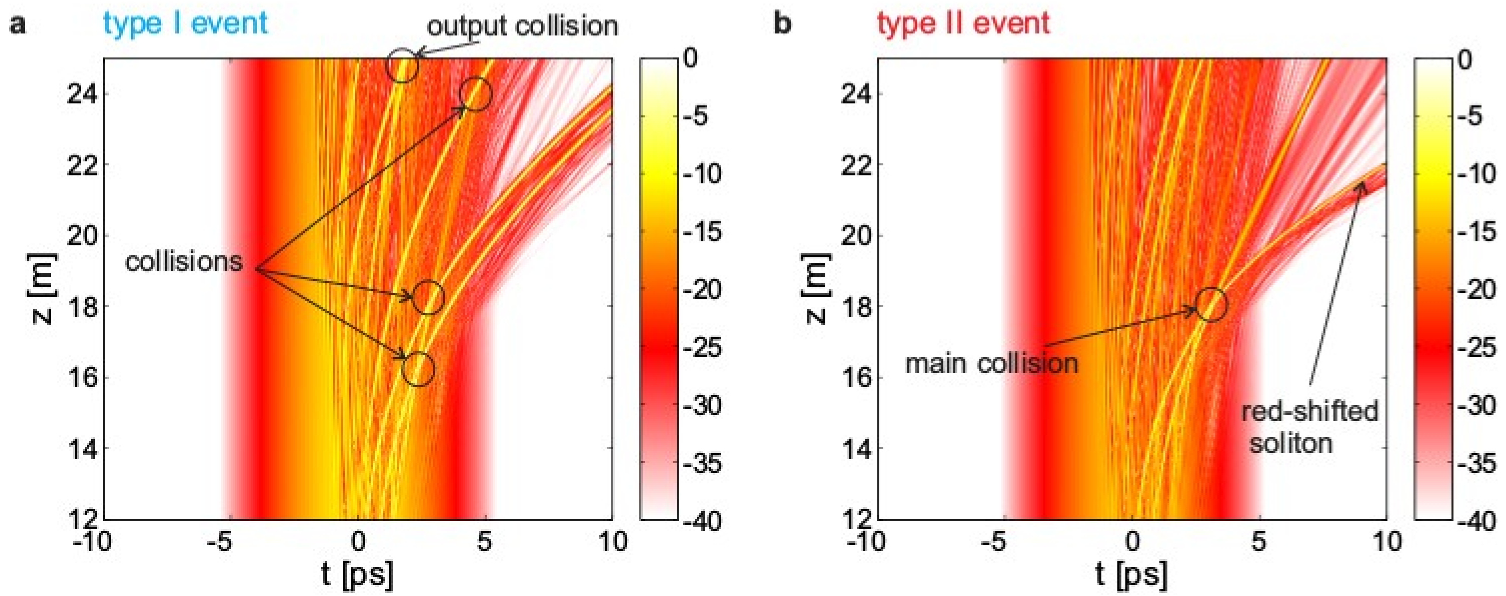

Again the landscape :

(more complicated)

A Armaroli, CC, F Biancalana, Geometric origin of rogue solitons in optical fibres, arXiv:1406.5966

NLS in the time domain

$$i\frac{\partial u}{\partial z} + \frac{1}{2}\frac{\partial^2 u}{\partial t^2} + |u|^2 u = 0,$$

$$H(z) = \int_{-\infty}^{\infty} \mathcal{H}(z,t)\mathrm{d}t$$

with $\mathcal{H}(z,t) \equiv \mathcal{H}_K + \mathcal{H}_{NL}$, $\mathcal{H}_K \equiv |u_t|^2/2$ and $\mathcal{H}_{NL} \equiv -|u|^4/2$.

$$i\frac{\partial U}{\partial Z} + \sum_{k\geq 2} \frac{i^k}{k!}\beta_k \frac{\partial^k U}{\partial T^k}$$

$$+\gamma\left(1 + i\tau_{\text{shock}}\frac{\partial}{\partial T}\right) U \int_0^{\infty} R(T')|U(T-T')|^2 \mathrm{d}T' = 0$$

Interacting solitons models

$$i\frac{\partial u}{\partial z} + \frac{1}{2}\frac{\partial^2 u}{\partial t^2} + |u|^2 u = 0,$$

$$u(z,t) = \sum_{k=1}^{N} u_k(z,t)$$

$$u_k(z,t) = 2\nu_k \operatorname{sech}[2\nu_k(t-\xi_k)]e^{i2\mu_k(t-\xi_k)+i\delta_k}$$

N-soliton model

$$\dot{\nu}_k = 16\nu_k^2\left(S_{k,k-1} - S_{k,k+1}\right)$$

$$\dot{\mu}_k = -16\nu_k^2\left(C_{k,k-1} - C_{k,k+1}\right)$$

$$\dot{\xi}_k = 2\mu_k - 4\left(S_{k,k-1} - S_{k,k+1}\right)$$

$$\dot{\delta}_k = 2(\nu_k^2 + \mu_k^2) - 8\mu_k\left(S_{k,k-1} + S_{k,k+1}\right) + 24\nu_k\left(C_{k,k-1} + C_{k,k+1}\right)$$

$$S_{k,n} = e^{|\beta_{kn}|}\nu_n \sin s_{kn}\phi_{kn}$$

$$C_{k,n} = e^{|\beta_{kn}|}\nu_n \cos\phi_{kn}$$

$$\beta_{kn} = 2\nu_k\left(\xi_k - \xi_n\right)$$

$$\phi_{kn} = \delta_k - \delta_n - 2\mu_n\left(\xi_k - \xi_n\right)$$

and $s_{kn} = \mathrm{sgn}\left[\beta_{kn}\right]$.

We solve these equation by a standard routine

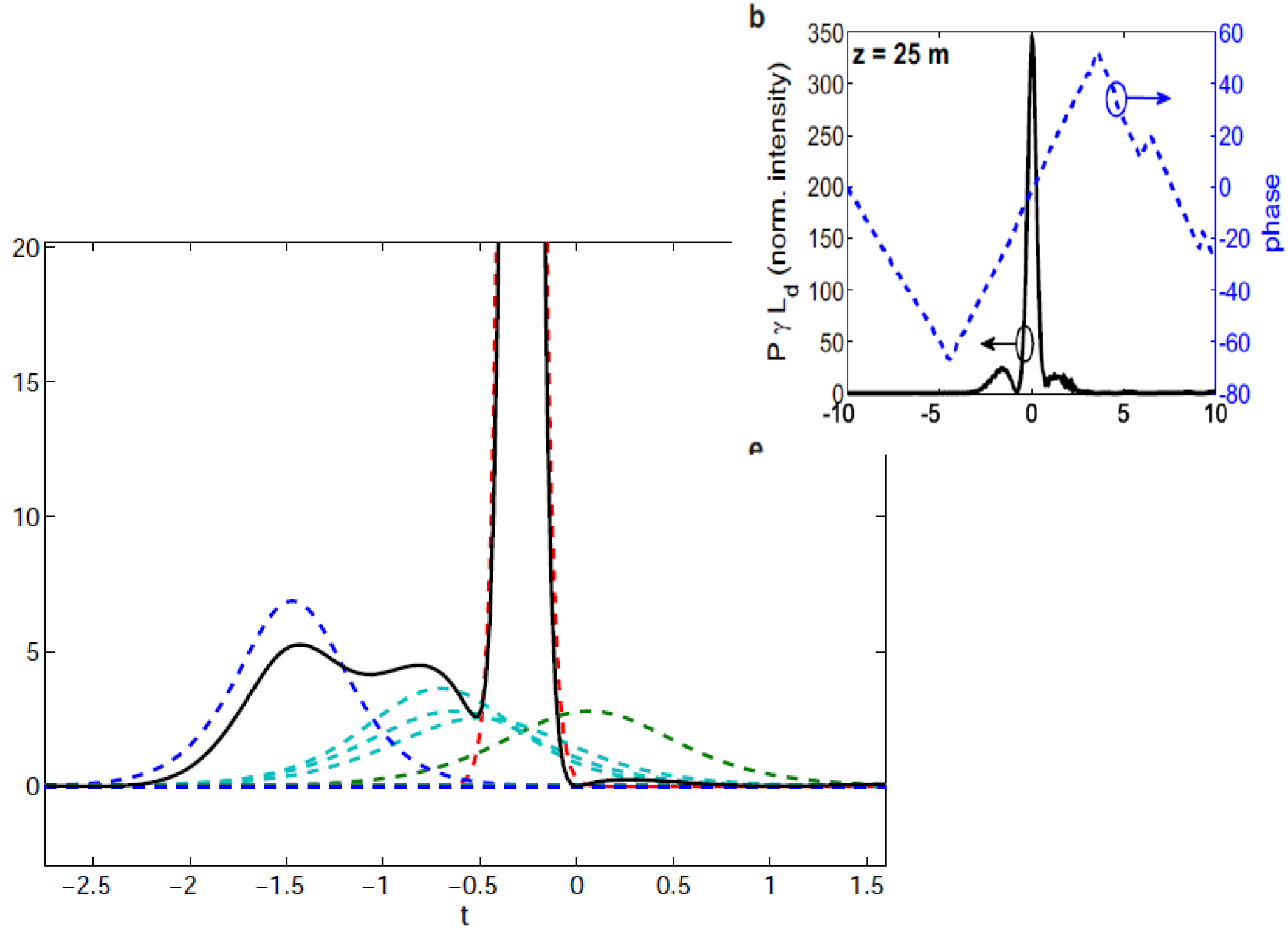

Figure : Full field for the previous exceptional solution (zoom). The small solitons in the vicinity of the giant one are not well-separated.

Solutions

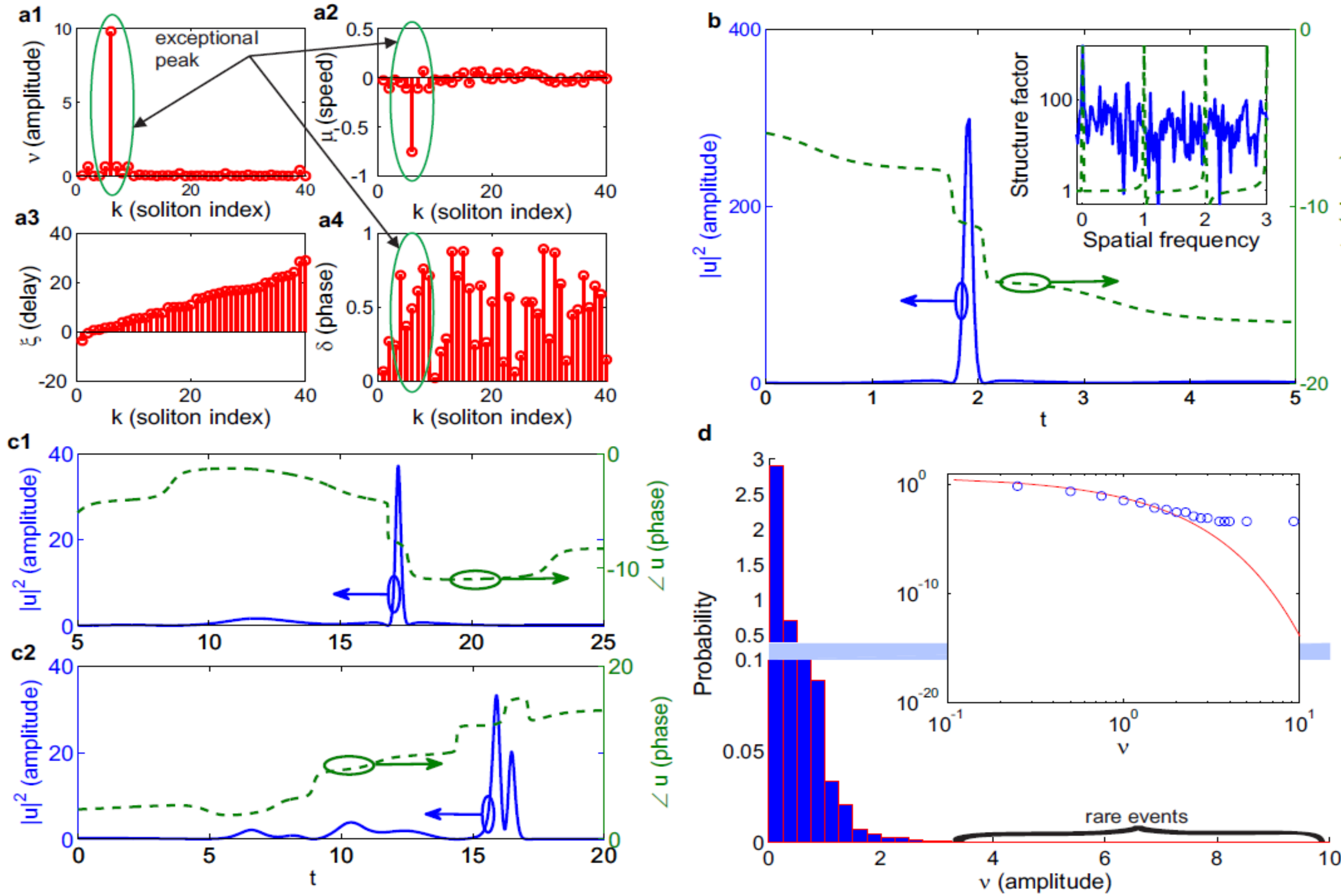

A Armaroli, CC, F Biancalana, arXiv:1406.5966

Link the statistical distribution of equilibria with the occurrence of rare rogue events
(a geometric origin of rogue waves)

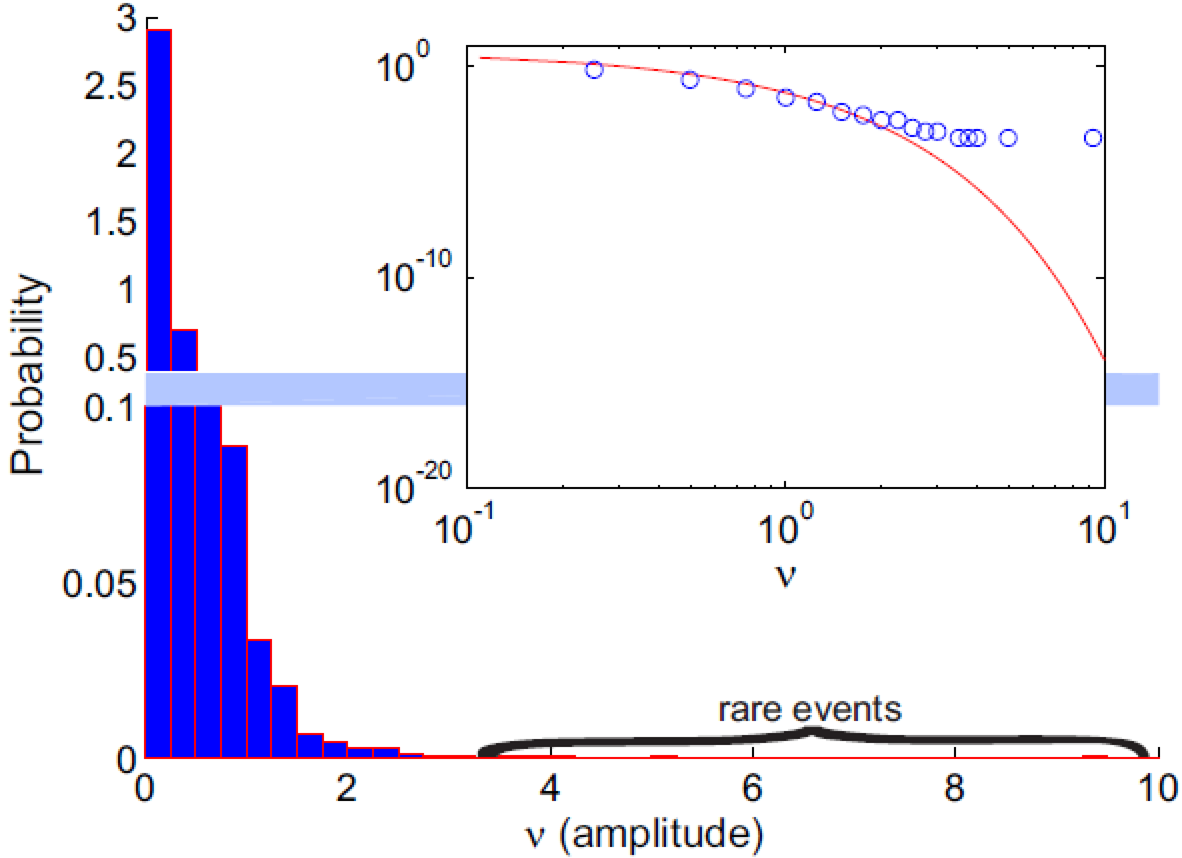

Comparing the saddle points with the soliton profiles

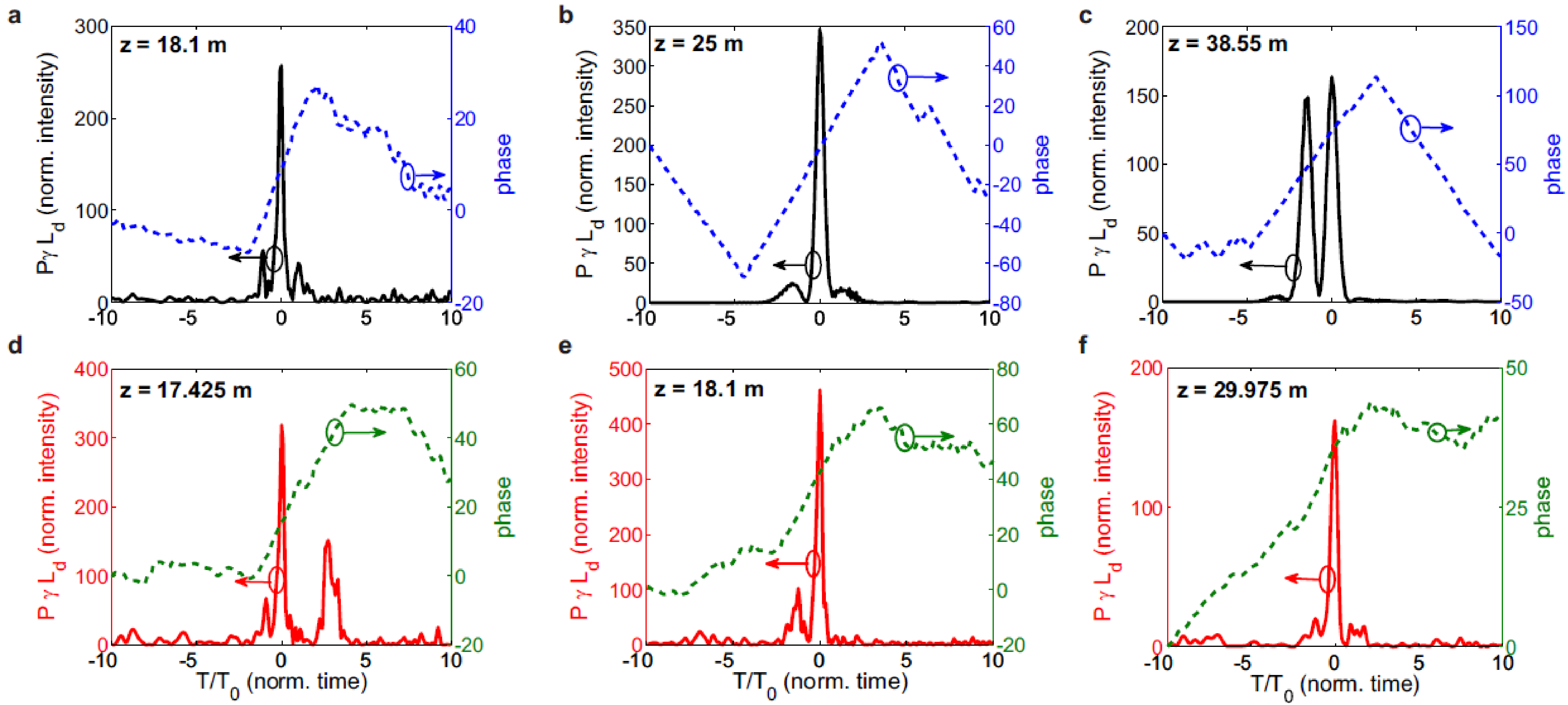

Energy minima Vs dynamics

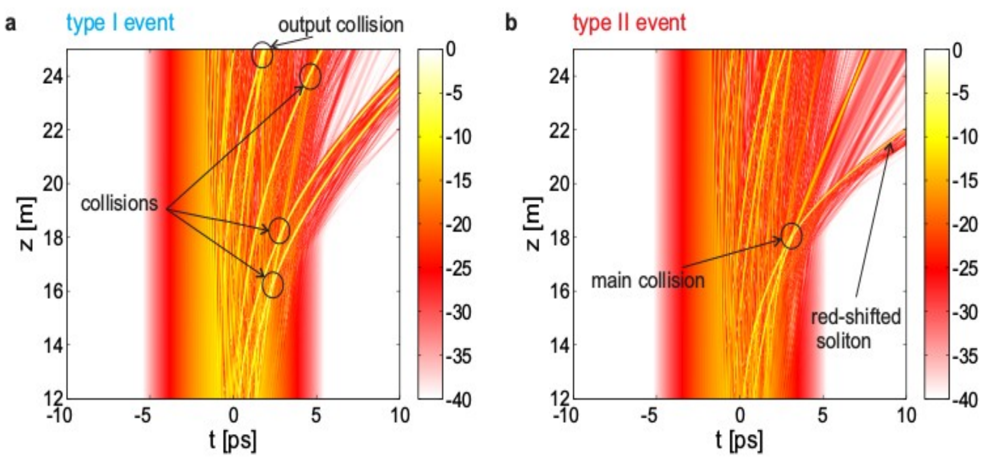

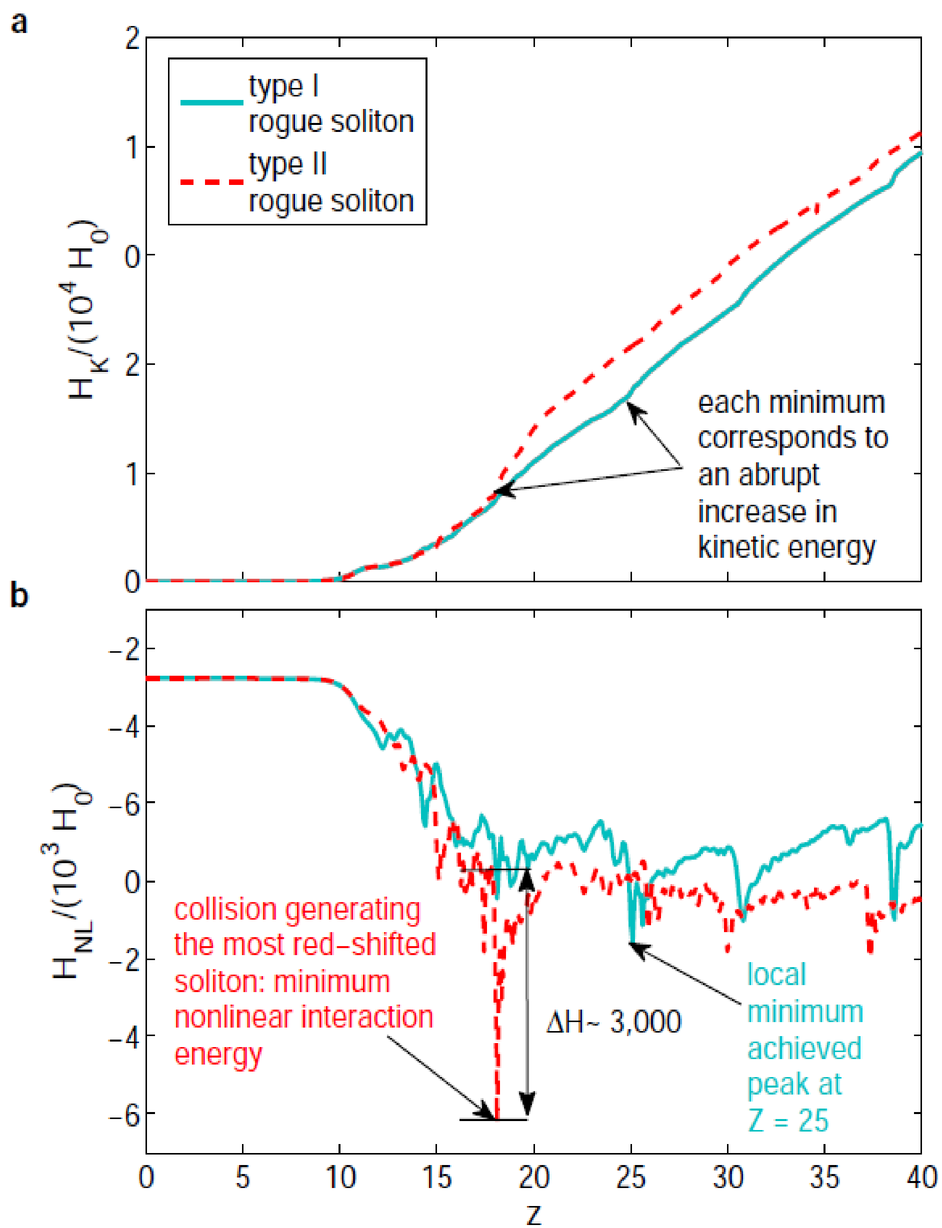

The lowest energy solution